REPORT DOCUMENTATION PAGE

Form Approved
OMB No. 0704-0188

1. REPORT DATE *(DD-MM-YYYY)*	2. REPORT DATE	3. DATES COVERED *(From - To)*
31-07-2002	Final Report July 31, 2002	May 1, 1998 - April 30, 2002

4. TITLE AND SUBTITLE

Electron Emitters

5a. CONTRACT NUMBER

5b. GRANT NUMBER

N00014-98-1-0571

5c. PROGRAM ELEMENT NUMBER

6. AUTHOR(S)

Yonhua Tzeng

5d. PROJECT NUMBER

5e. TASK NUMBER

5f. WORK UNIT NUMBER

7. PERFORMING ORGANIZATION NAME(S) AND ADDRESS(ES)

Auburn University
Department of Electrical and Computer Engineering
Auburn, AL 36849

8. PERFORMING ORGANIZATION REPORT NUMBER

9. SPONSORING/MONITORING AGENCY NAME(S) AND ADDRESS(ES)

Dr. Colin E. Wood
ONR312, Office of Naval Research
Ballston Center Tower One, 800 North Quincy St.
Arlington, VA 22217-5660

10. SPONSOR/MONITOR'S ACRONYM(S)

11. SPONSORING/MONITORING AGENCY REPORT NUMBER

12. DISTRIBUTION AVAILABILITY STATEMENT

Approved for public release.

13. SUPPLEMENTARY NOTES

14. ABSTRACT

This is the final report for the Grant N00014-98-1-0571. During the grant period, one Ph.D. and two M.S. degrees were awarded, three patents were awarded, fifteen presentations and publications were made, organization of two technical conferences was accomplished. A list of these accomplishments is reported and five publications that were not previously reported are attached with this final report.

15. SUBJECT TERMS

Electron Emitter, Carbon Nanotube, Diamond, Cubic Boron Nitride

16. SECURITY CLASSIFICATION OF:			17. LIMITATION OF ABSTRACT	18. NUMBER OF PAGES	19a. NAME OF RESPONSIBLE PERSON
a. REPORT	b. ABSTRACT	c. THIS PAGE			Yonhua Tzeng
UU	UU	UU	None	70	19b. TELEPONE NUMBER *(Include area code)* (334) 844-1869

Final Report

1. Report Date: **31-07-2002**
2. Report Type: **Final Report**
3. Dates Covered: **May1, 1998 – April 30, 2002**
4. Title: **Electron Emitters**
5. Funding Number: **Grant N00014-98-1-0571**
6. Author: **Yonhua Tzeng, Ph.D., Professor of Electrical and Computer Engineering**
7. Performing Organization: **Department of Electrical and Computer Engineering, Auburn University, 200 Broun Hall, Auburn, AL 36849**
8. Performing Organization Report Number: blank
9. Sponsoring/Monitoring Agency: **Dr. Colin E. Wood, ONR312, Office of Naval Research, Ballston Center Tower One, 800 North Quincy St., Arlington, VA 22217-5660**
10. Sponsor/Monitor's Acronym(s): blank
11. Sponsoring/Monitoring Agency Report Number: blank
12. Distribution: **Approved for public release.**
13. Supplementary Notes: blank
14. Abstract: **This is the final report for the Grant N00014-98-1-0571. During the period of May1-1998- April 30, 2002, one Ph.D. and two M.S. degrees were awarded, three patents were awarded, fifteen presentations and publications were made, organization of two technical conferences as Chairman or Co-Chairman was accomplished. A list of these accomplishments is reported and five publications that have not been previously reported are attached with this final report.**
15. Subject Terms: **Electron Emitter, Carbon Nanotube, Diamond, Cubic Boron Nitride**

Accomplishments:

1. Students Supported and Graduated:

One Ph.D. student and two M.S. students who were partially supported by this grant have graduated during the grant period.

2. Patents Awarded:

"Method of Synthesizing Cubic Boron Nitride Films," U.S. patent, #6,153,061, November 28, 2000, Y. Tzeng and H.B. Zhu.

"Method for Smoothing CVD Diamond," U.S. patent #6,284,315, September 4, 2001, Y. Tzeng (Based on a contract funded by Naval Air Warfare Center).

"Structures with High Number Density of Carbon Nanotubes and 3-Dimensional Distribution," U.S. Patent allowed, July 2002, Zheng Chen and Yonhua Tzeng .

3.Publications:

"Carbon-Nanotube Cold Cathodes As Non-Contact Electrical Couplers", Y. Tzeng, C. Liu and Y. Chen, presented at ICNDST-8, Australia, July 21, 2002 and submitted for publication in *Diamond and Related Materials.*

"Characteristics and Applications of Electrical Contacts Between Aligned Carbon Nanotube Coatings and Small Movable Gold Electrodes", Y. Tzeng, C. Liu and Y. Chen, presented at ICNDST-8, Australia, July 21, 2002 and submitted for publication in *Diamond and Related Materials..*

"Microwave Plasma CVD of Diamond and Nanodiamond Coatings In Vapor Mixtures of Methanol and Ethanol And Applications To Cold Cathodes", Y. Tzeng, C. Liu and Y. Chen, presented at ICNDST-8, Australia, July 21, 2002 and submitted for publication in *Diamond and Related Materials.*

"Microwave Plasma Assisted Brazing of Carbon Nanotubes and Deposition of Carbon Films on Iron Electrodes for Applications as Electron Field Emitters" Yonhua Tzeng, Chao Liu, and Calvin Cutshaw, *Proceedings of the Sixth Applied Diamond Conference/Second Frontier Carbon Technology Joint Conference (ADC/FCT 2001),* NASA/CP-2001-210948, Y. Tzeng et al, editors, pp. 736-741, August 6, 2001, Auburn, Alabama.

"Hysteresis of Electron Field Emission from Single-Walled Carbon Nanotubes Brazed on Iron Substrates" Chao Liu, Calvin Cutshaw and Yonhua Tzeng, *Proceedings of the Sixth Applied Diamond Conference/Second Frontier Carbon Technology Joint Conference (ADC/FCT 2001),* NASA/CP-2001-210948, Y. Tzeng et al, editors, pp. 742-746, August 6, 2001, Auburn, Alabama.

"Hot-Filament Assisted Fabrication of Carbon Nanotube Electron Emitters," Yonhua Tzeng, Chao Liu and Zheng Chen, *Mat. Res. Soc. Symp. Proc.* Vol. 621. R7.5.1-R7.5.7, April 24-28, 2000, San Francisco, CA.

"Fabrication and Applications of Microstructured Ni-C Electrodes with High-Density Carbon-Nanotube Coatings," Zheng Chen, Yonhua Tzeng, Chao Liu, and Calvin Cutshaw, *Mat. Res. Soc. Symp. Proc.* Vol. 621. R7.4.1-R7.4.4 , April 24-28, 2000, San Francisco, CA.

"Electron Emission from Microwave Plasma CVD Carbon Nanotubes," Yonhua Tzeng, Chao Liu, and Zheng Chen, *Mat. Res. Soc. Symp. Proc.* Vol. 621. R7.3.1-R7.3.6 , April 24-28, 2000, San San Francisco, CA.

"Low Temperature CVD Carbon Nanotubes on Glass Plates for Flat Panel display applications," Y. Tzeng, C. Liu, and Z. Chen, ," *Mat. Res. Soc. Symp. Proc.* Vol. 621.

Q2.2.1-Q2.2.5 , April 24-28, 2000, San Francisco, CA.

"Carbon Nanotube Coatings for Electron Emitter Applications," Y. Tzeng, C. Liu, C. Cutshaw, and Z. Chen, Presented in the *Seventh International Conference on New Diamond Science and Technology*, July 24-28, 2000, Hong Kong, China.

"CVD Diamond Grown by Microwave Plasma in Mixtures of Acetone/ Oxygen and Acetone/ Carbon Dioxide," Diamond and Related Materials 8 (1999) 1393-1401, Tsan-Heui Chein and Yonhua Tzeng.

"Synthesis of Diamond in High Power-density Microwave Methane/ Hydrogen/ Oxygen Plasmas at Elevated Substrate Temperatures," Diamond and Related Materials 8 (1999) 1686-1696, Tsan-Heui Chein, Jin Wei, and Yonhua Tzeng.

"Hot-Filament Assisted Deposition of Diamond in the Vapor of Methanol-Based Liquid Solutions," Proceedings of ADC/FCT 1999, pp.420-424, August 31 – September 4, 1999, Tsukuba, Japan, Y. Tzeng.

"Microwave Plasma Enhanced Chemical Vapor Deposition of Diamond in the Vapor of Methanol-Based Liquid Solutions," Proceedings of ADC/FCT 1999, pp.20-24, August 31 – September 4, 1999, Tsukuba, Japan, Y. Tzeng.

"Electron-assisted Deposition of Cubic Boron Nitride by RF Magnetron Sputtering, " Diamond and Related Materials 8 (1999) 1402-1405, Y. Tzeng and H. Zhu.

4.Conference Organization for Technical Exchanges:

Conference Chairman, Sixth Applied Diamond Conference/ Second Frontier Carbon Technology Joint Conference 2001, Auburn University Hotel and Dixon Conference Center, Alabama USA, August 4-10, 2001.

Organizing Committee Co-Chairman, Applied Diamond Conference/ Frontier Carbon Technology Joint Conference 1999, Tsukuba, Japan, August 31 – September 4, 1999.

5. Five Publications Are Attached:

1. "Carbon-Nanotube Cold Cathodes As Non-Contact Electrical Couplers", Y. Tzeng, C. Liu and Y. Chen, presented at ICNDST-8, Australia, July 21, 2002 and submitted for publication in *Diamond and Related Materials.*

2. "Characteristics and Applications of Electrical Contacts Between Aligned Carbon Nanotube Coatings and Small Movable Gold Electrodes", Y. Tzeng, C. Liu and Y. Chen, presented at ICNDST-8, Australia, July 21, 2002 and submitted for publication in *Diamond and Related Materials..*

3. "Microwave Plasma CVD of Diamond and Nanodiamond Coatings In Vapor Mixtures of Methanol and Ethanol And Applications To Cold Cathodes", Y. Tzeng, C. Liu and Y. Chen, presented at ICNDST-8, Australia. July 21, 2002 and submitted for publication in *Diamond and Related Materials.*

4. "Microwave Plasma Assisted Brazing of Carbon Nanotubes and Deposition of Carbon Films on Iron Electrodes for Applications as Electron Field Emitters" Yonhua Tzeng, Chao Liu, and Calvin Cutshaw, *Proceedings of the Sixth Applied Diamond Conference/Second Frontier Carbon Technology Joint Conference (ADC/FCT 2001),* NASA/CP-2001-210948, Y. Tzeng et al, editors, pp. 736-741. August 6, 2001, Auburn, Alabama.

5. "Hysteresis of Electron Field Emission from Single-Walled Carbon Nanotubes Brazed on Iron Substrates" Chao Liu, Calvin Cutshaw and Yonhua Tzeng, *Proceedings of the Sixth Applied Diamond Conference/Second Frontier Carbon Technology Joint Conference (ADC/FCT 2001),* NASA/CP-2001-210948. Y. Tzeng et al, editors, pp. 742-746, August 6, 2001, Auburn, Alabama.

Presented in ICNDST-8 and submitted to Diamond and Related Materials

Carbon-Nanotube Cold Cathodes As Non-Contact Electrical Couplers

Y. Chen, C. Liu, and Y. Tzeng

Department of Electrical and Computer Engineering

Auburn University, Auburn, Alabama 36849 (USA)

Abstract

When two carbon-nanotube coated electrodes are placed at a small distance from each other, electron emission from carbon nanotubes allows a DC or AC electrical current to flow between these two electrodes. The voltage drop across these two electrodes depends on the electric field needed for emitting electrons necessary for carrying electric current and the distance between these two electrodes. This electrical coupler may find applications to high-voltage circuits, which operate at voltages of a much larger value than what is needed across the electrical coupler to supply the current. Because of the non-contact nature of this class of electrical coupler, two electrodes are allowed to move with respect to each other while keeping the gap spacing constant and allowing the DC or AC power to be coupled from one electrode to the other..

* Corresponding author's e-mail address: tzengy@eng.auburn.edu

1. Introduction

Carbon nanotube is among the most promising cold cathode materials because of its excellent electrical, thermal, and mechanical properties, such as high aspect ratio, high mechanical strength, and high resistance to chemical and physical attacks [1-5]. Low threshold and turn-on electric fields for field emission of electrons, as well as high emission current densities have been demonstrated. In this paper, carbon nanotube cold

cathodes will be explored and applied as high-voltage rectifiers and full-wave non-contact power couplers. These applications need cold cathodes with very high electron field emission current density and very low turn-on electric field. The small the voltage drop across the electrodes and the larger the current allowed per square centimeter, the better the device is used for non-contact power coupling.

2. Experimental details

2.1 Fabrication *of carbon nanotube coated electrodes*

Iron catalyst was sputtered on silicon substrates followed by heating in air at 300°C for 8 hours. Thermal CVD of carbon nanotubes was performed in a vacuum furnace filled with a gas mixture of acetylene and argon at a pressure of 70 torr. The flow rates for argon and acetylene were 75 sccm and 20 sccm, respectively. Before the gas mixture was fed into the furnace, the substrate was heated to 700°C in vacuum and the temperature was remained constant during the 20 minutes growth of carbon nanotubes.

Single walled carbon nanotubes were suspended in a solution and then coated on silicon substrates. After the solution vaporized, these single walled carbon nanotube coated silicon substrates were used as electrodes. Clean silicon substrates were used as the anode when electron emission from clean silicon electrodes is not desirable.

2.2 Current-voltage characteristics measurement

When electron emission characteristics, i.e. the emission current vs electric field plot, are measured, a space was place between a clean silicon and a carbon nanotube coated electrode and a computer controlled DC power supply supplies voltages to the gap allowing current to flow through the gap and a resistor. A pico-ammeter was used to measure the emission current with data fed to a computer for further processing. The

electrodes were placed inside a high-vacuum chamber for the electron emission measurement.

Shown in Figure 1 is the setup for power coupling measurements. A 60 Hz AC was applied across two electrodes placed at a fixed distance and a current limiting resistor. The waveform for the voltage across these two electrodes and that for the current flowing through the gap between these two electrodes were recorded using an oscilloscope. For rectifying operation, one electrode was coated with carbon nanotube while the counter electrode was a clean silicon. For two-way coupling of electric power, both electrodes were coated with carbon nanotubes.

3. Results and discussion

3.1 Rectifying electrical power coupling

When electrical current is to be allowed to flow in only one direction, a carbon nanotube coated electrode was used as the cathode while a clean silicon substrate was used the anode. A 60 Hz AC power supply was used to power the circuit.

3.1.1 Single walled carbon nanotube coated cathode as a rectifier

Shown in Figure 2 (a) is the oscilloscope trace of a half-wave rectified 60 Hz electron current that flew from a single walled carbon nanotube coated cathode to a clean anode when a power supply was first turned on to 606 Volts. There was no electron current flowing from the clean silicon to the carbon nanotube coated cathode.

After a few minutes, for example, oscilloscope traces shown in Figure 2 (b-d), electron current started to flow from the originally clean silicon electrode towards the carbon nanotube coated electrode. The electron current originating from the clean silicon electrode can be seen as the smaller negative part of the waveforms. The electron

current originating from the silicon electrode first increased with time. After hours of operation, both electron current from carbon nanotube coated electrode and that from the silicon electrode decresed and stabilized as shown in Figure 2(d).

The on-set of electron emission from the silicon electrode, that was not intentionally coated with carbon nanotubes, was actually caused by the coating with carbon nanotubes that were forced to fly from the carbon nanotube coated cathode to the clean silicon electrode by a strong electro-static force.

Shown in Figure 2(e) is the electron field emission characteristics of the single walled carbon nanotube coated electrode. Shown in Figure 2(f) is the electron field emission characteristics of the originally clean silicon electrode. A negative voltage was applied to the clean silicon electrode to force some loose or broken carbon nanotubes to fly across the gap and get deposited on the originally clean silicon electrode. The on-set of electron emission from the originally clean silicon electrode was similar to that of the single walled carbon nanotube coated electrode indicating that some broken pieces or loose carbon nanotubes on the cathode was forced by the electric field to fly and coat on the silicon substrate.

3.1.2 Multiple walled carbon nanotube coated cathode as a rectifier

Shown in Figure 3 (a) is the oscilloscope trace of a half-wave rectified 60 Hz electron current that flew from a multiple walled carbon nanotube coated cathode to a clean anode when a power supply was first turned on to 606 Volts. There was no electron current flowing from the clean silicon to the carbon nanotube coated cathode.

After four hours of operation, there was no electron emission from the clean silicon electrode as shown in Figure 3(b). This indicated that adhesion of CVD multiple

walled carbon nanotubes on the substrate was stronger than that of single walled carbon nanotubes on the substrate The applied voltage was raised from 606 Volts to 2373 Volts and almost immediately the waveform shown in Figure 3(c) shows electron current flowing from both the originally clean silicon electrode and the carbon nanotube coated electrode. It took 2372 V applied voltage instead of just 606 V to break pieces of carbon nanotubes and other carbon particles loose from the CVD carbon nanotube coated electrode. The electron current from the silicon electrode remained stable for three hours as shown in Figure 3(d)

The on-set of electron emission from the silicon electrode, that was not intentionally coated with carbon nanotubes, was actually caused by the coating with carbon nanotubes and non-carbon nanotube that were forced to fly from the carbon nanotube coated cathode to the clean silicon electrode by a strong electro-static force.

Shown in Figure 3(e) is the electron field emission characteristics of the multiple walled carbon nanotube coated electrode. Shown in Figure 3(f) is the electron field emission characteristics of the originally clean silicon electrode after applying 2373 volts of 60 Hz AC across the electrodes and a resistor. The on-set of electron field emission from the originally clean silicon electrode was higher than the CVD coated one. This indicated that there were some non-carbon nanotube carbons that got forced to leave the carbon nanotube coated electrode to the clean silicon. These carbon particles took a higher electric for the on-set of electron field emission.

3.2 Full-wave non-contact power coupling

Both electrodes were coated with carbon nanotubes so that electron current can flow in both directions.

3.2.1 Single walled carbon nanotube coated full-wave coupler

Shown in Figure 4 are two oscilloscope traces for the applied sinusoidal voltage and the electron current single showing the current flowing in both directions. The electron current flow in two direction were not of the same magnitude because two electrodes were not evenly coated by single walled carbon nanotubes.

3.2.2 Multi-walled carbon nanotube coated full-wave coupler

Shown in Figure 5 (a-d) are four oscilloscope traces for the electron current flowing through the gap between two electrodes coated with CVD multi-walled carbon nanotubes. The electric power can be coupled in both directions. As shown in Figure 5 (d), the electron emission current actually increased with time of operation as can be compared with that shown in Figure 5 (a). Strong electric fields between two electrodes force loose or broken particles and nanotubes to fly from one side to the other. These small pieces may be the cause of the increasing of electron emission current with time. The alternative exposure of carbon nanotubes to electron beams from the counter electrodes may also contribute to the time-varying electron emission current density. Shown in Figure 6 is the electron emission current from both electrodes as a function of time. The electron emission currents increased with time of operation.

3.3 Potential applications of carbon nanotube couplers as vacuum opening/closing switches

When the effective electrical coupling resistance is minimized, the electrical coupler may serve as an electrical switch that is at its closed position with the minimum voltage drop across two electrodes being much smaller than the applied high-voltage in the circuit. This class of switches may find many applications for high voltage circuits

operating in the space or in a vacuum. This switch may be opened by increasing the distance between two carbon nanotube coated electrodes. A properly patterned CNT coating and a patterned couner electrode can move with each other in parallel in such a way as to increase the distance between patterned carbon nanotubes on one electrode with respect to a patterned counter electrode. When the distance between the CNT cathode and the anode is so large that carbon nanotubes becomes subjected to a electric field that is below the on-set threshold for electron emission. The coupling of electrical current is, therefore, disabled and the switch is effectively opened

4. Conclusions

Application of carbon nanotube coated electrodes as half-wave rectifier and full-wave non-contact couplers has been studied. Adhesion of carbon nanotubes to substrate is a critical issue for the rectifying applications. Unless the anode can be protected from unwanted carbon particles and broken loose carbon nanotubes that are attracted to the anode by strong electric fields, the anode will not be able to sustain strong negative voltage before it start to "leak" electron current. For full-wave power coupling, the cross contamination is not a negative issue. As a matter of fact, it might have helped increase the electron emission current, and, therefore, decrease the voltage drop across the electrodes during operation. When a higher voltage is applied and a smaller gap spacing is adopted, the voltage drop across two electrodes will decrease and the current waveform will become closer to the applied sinusoidal waveform.

References

1. Yahachi Saito and Sashiro Uemura: "Field emission from carbon nanotubes and its application to electron sources", Carbon, 85, 7, 2000, p169.

2. W. Zhu et al.: "Large current density from carbon nanotube field emitters", Appl. Phys. Lett., 75, 6, 1999, p873.

3. O. Gröning et al.: "Field emission properties of carbon nanotubes", J. Vac. Sci. Technol. B, 18(2), 2000, p665.

4. R. Saito, G. Dresselhaus, and M. S. Dresselhaus: Physical Properties of Carbon Nanotubes, Imperial College Press, London, 1999 Journal of Applied Physics, Volume 85, Number 7, 1999, p3832.

5. Kenneth A. Dean and Babu R. Chalamala: "Field emission microscopy of carbon nanotube caps", J. Appl. Phys., 85, 7, 1999, p3832.

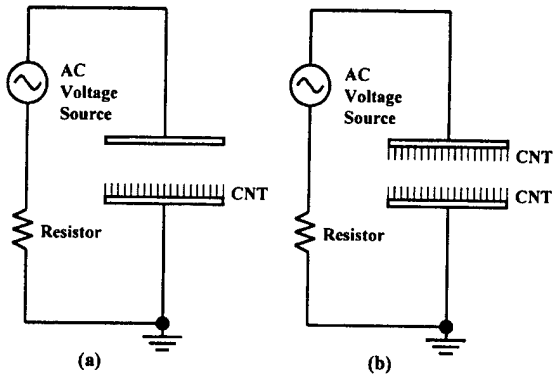

Figure 1. Schematic diagrams of setups for measuring rectifying and full-wave power coupling.

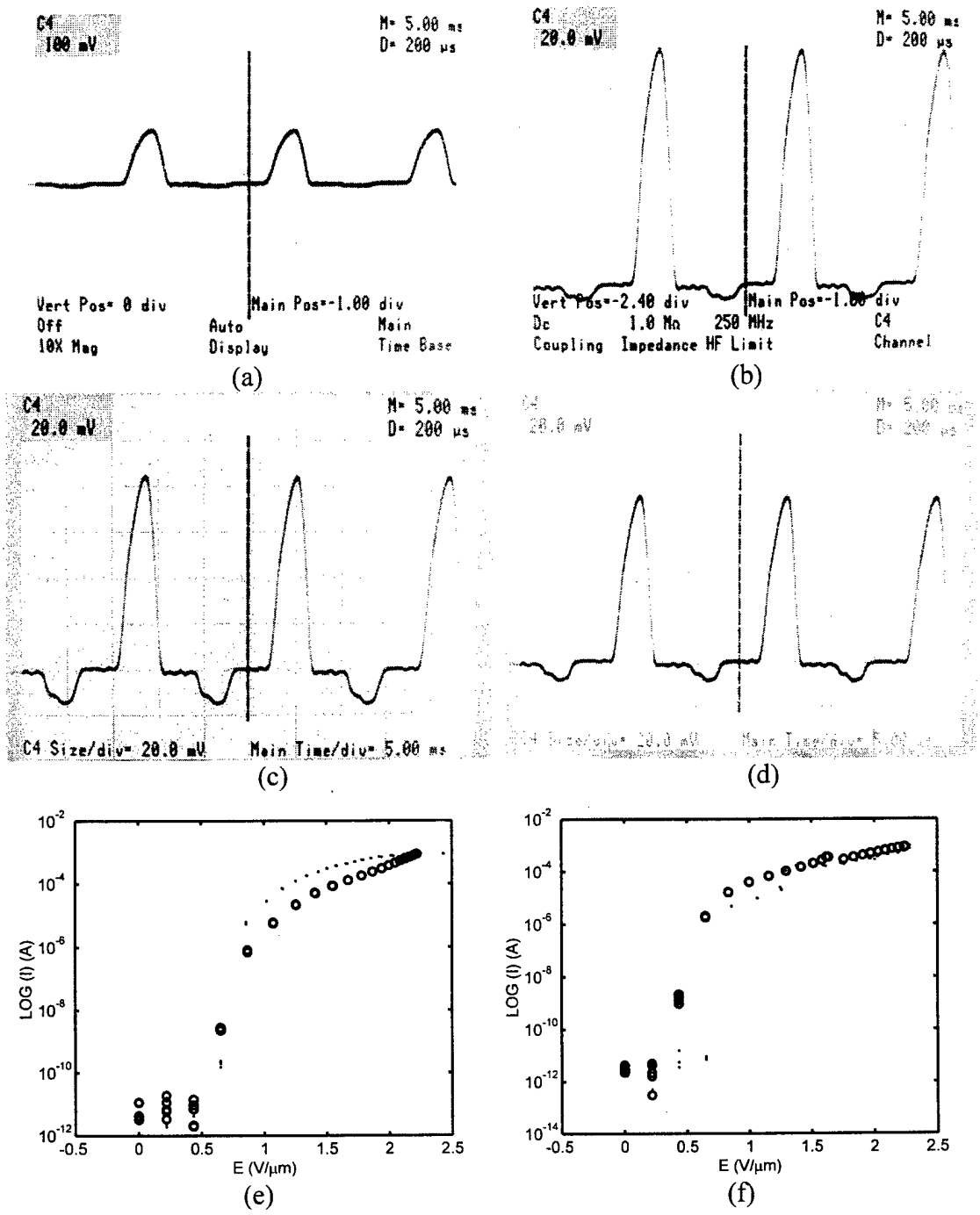

Figure 2. Electron field emission characteristics of single walled carbon nanotube: (a) Rectifying electron current when the applied voltage was first turned on. (b) After 15 minutes operation. (c) After 2 hours operation. (d) After 16 hours operation. (e) Current-electric field plot for the carbon nanotube coated cathode. (f) Current-electric field plot for the originally clean silicon electrode. Dot: Current vs. Increasing electric field; Circle: Current vs. Decreasing electric field.

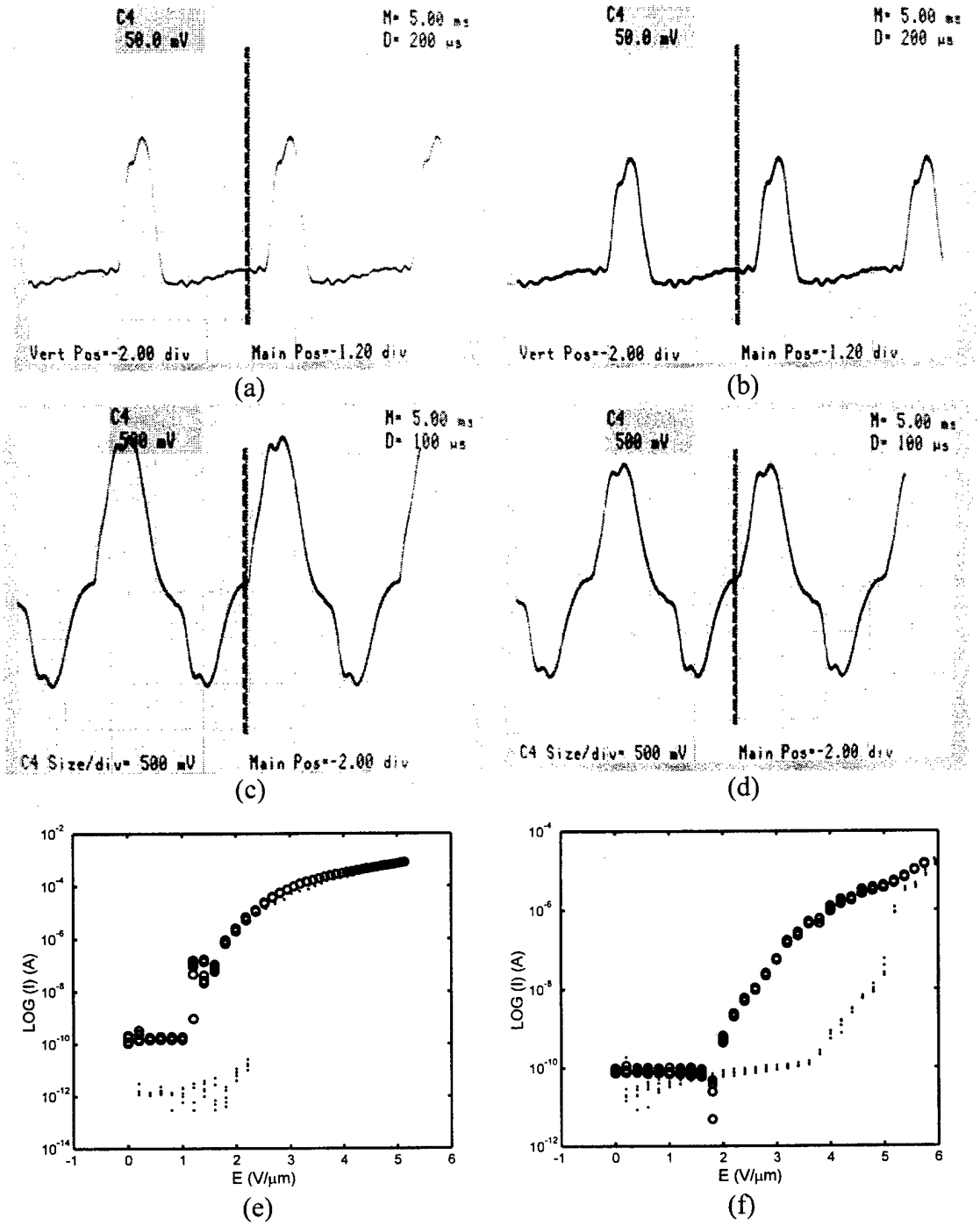

Figure 3. Electron field emission characteristics of multi-walled carbon nanotube: (a) Rectifying electron current when the applied voltage was first turned on. (b) After 4 hours operation. (c) Applied voltage was increased from 606 volts to 2373 volts. (d) After 3 hours operation at 2373 volts. (e) Current-electric field plot for the multi-walled carbon nanotube coated cathode. (f) Current-electric field plot for the originally clean silicon electrode. Dot: current vs. increasing electric field; Circle: current vs. decreasing electric field.

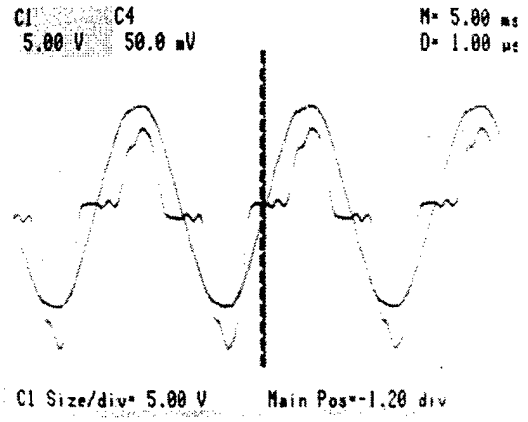

Figure 4. Electrical power coupling between two silicon electrodes both coated with single walled carbon nanotubes

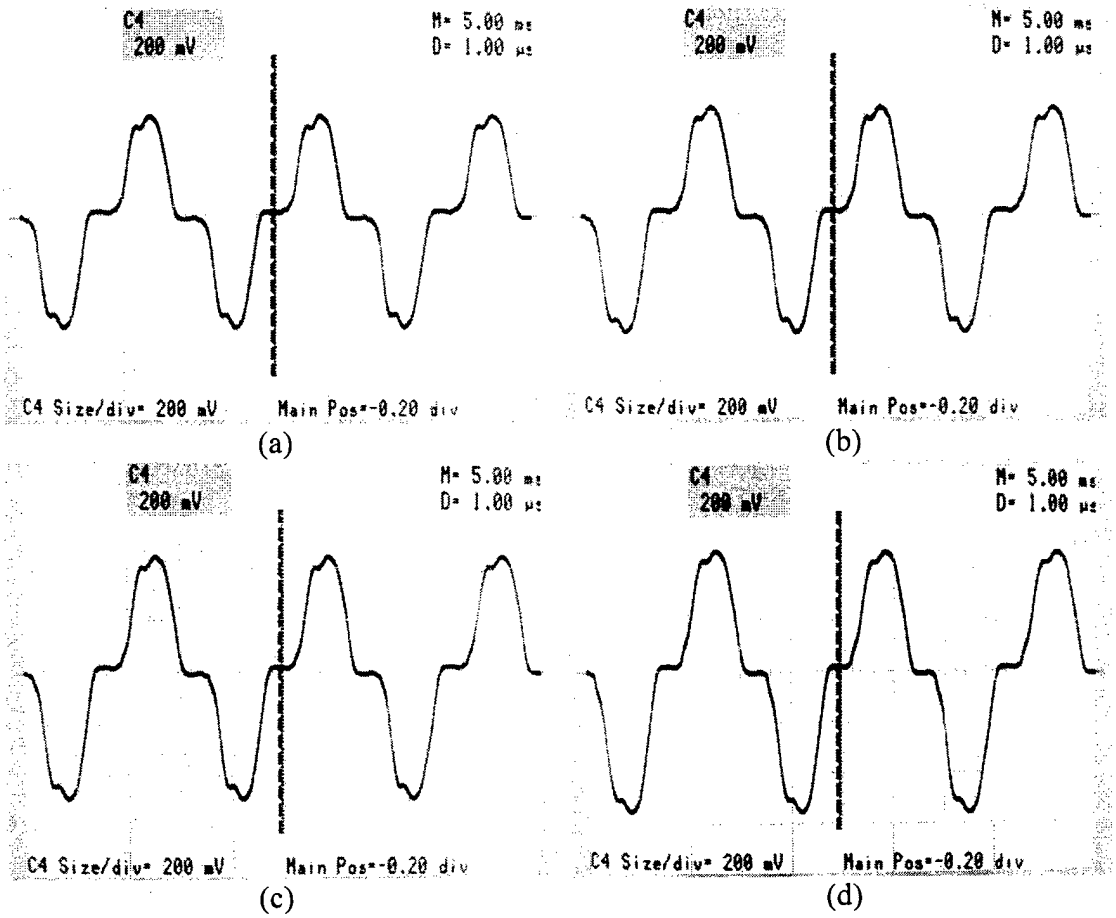

Figure 5. Electrical power coupling between two silicon electrodes both coated with multiple walled carbon nanotubes: (a) Electron current when the power supply of 1193 volts was first turned on. (b) After 25 minutes operation. (c) After 2 hours and 30 minutes operation. (d) After 9 hours operation.

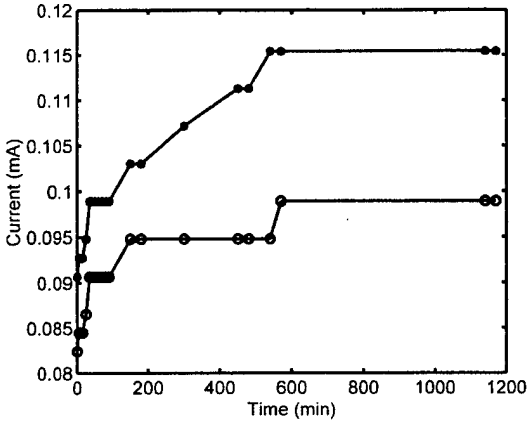

Figure 6. Electron emission current from two electrodes powered by 1193 volts showing increasing current with time.

Presented in ICNDST-8 and submitted to Diamond and Related Materials

Characteristics and Applications of Electrical Contacts Between Aligned Carbon Nanotube Coatings and Small Movable Gold Electrodes

Y. Tzeng, Y. Chen, C. Liu, Calvin Cutshaw, and V. Krishnardula

Alabama Microelectronics Science and Technology Center

Department of Electrical and Computer Engineering

Auburn University, Auburn, Alabama 36849 (USA)

Abstract

Vertically aligned carbon nanotubes were grown on electrically conductive electrodes by means of thermal chemical vapor deposition in mixtures of argon and acetylene. These multi-wall carbon nanotubes are flexible, strong, and electrically conductive. Placing a metal electrode placed in contact with the carbon-nanotube coated electrode allows electrical current to flow between these two electrodes through carbon nanotubes. Electrical contact resistance and contact potential as a function of current loading, contact orientation, and depth of contact are reported. Potential applications of carbon-nanotube as electrical contacts between moving parts and sensing elements are discussed.

* Corresponding author's e-mail address: tzengy@eng.auburn.edu

Keywords: carbon nanotube, electrical contact

1. Introduction

Carbon nanotube (CNT) is among the most promising nanotechnology materials that may soon result in practical and commercial products that will greatly advance our modern standard of living. Besides its well known excellence in serving as a cold cathode allowing emission of electrons at low electric fields, carbon nanotube's

outstanding mechanical, thermal, chemical and physical properties make it one of the most studied carbon nano-structures in recent years.

Single-wall carbon nanotube (SWCNT) ropes typically have a low resistivity of 100-200 $\mu\Omega$·cm [1], which lies between a typical aluminum-copper-silicon interconnect line with a resistivity of 3.2 $\mu\Omega$·cm and a polysilicon interconnect line with a resistivity of 500 $\mu\Omega$·cm and is comparable with a high-quality carbon fiber with a resistivity of about 100 $\mu\Omega$·cm. Low measured resistivity has also been reported for multi-wall carbon nanotube (MWCNT) [2]. Boron doped MWCNT [7] was reported to have room-temperature resistivity down to 7.4×10^{-7} - 7.7×10^{-6} Ω·m as compared to pure nanotubes ($5.3 \times 10^{-6} - 1.9 \times 10^{-5}$ Ω·m), making the resistivity of the doped tubes comparable to that along the basal plane of graphite.

MWCNT was reported to be able to carry current of densities up to $10^9 - 10^{10}$ A/cm^2 and remain stable for an extended period of time at high temperature in air [3]. The sp^2 bonds in CNT lead to much higher threshold for electromigration than typical metallic interconnect materials such as aluminum. CNT shows resistivity anisotropy. The resistivity is lower in the aligned orientation with an anisotropy reported to be about 6-24 for a set of magnetically aligned SWCNT [1].

Although CNT can carry very high current density, it is known that by simply placing a CNT on a metal electrode we may measure the contact resistance to be on the order of kΩ or MΩ [3]. Tersoff [4] in his paper explained that high contact resistance between metal and CNT may be due to the unique electronic structure of the contact system, which results weak electronic coupling at the Fermi surface. He further suggested that the problem could be avoided by using a metal whose Fermi surface extends all the way to

the CNT Fermi point. An ideal candidate would be aluminum; however, aluminum oxide is not allowed. Bachtold et al. reported [5] that exposing a nanotube-Au contact locally by electron beam lowered the electric contact resistance substantially. The two-terminal-resistance decreased by four orders of magnitude from an initial value of > 100MΩ to ≈ 30 kΩ after a total exposure dose of 0.7 C/cm^2. Wei et al. [3] used a focused ion beam to deposit tungsten electrode onto CNTs and made the CNTs collapse partially, allowing the multilayers of the carbon nanotubes to contact the tungsten electrode directly. In this case, several layers of nanotubes carries current simultaneously making the contact resistance below 100Ω and mostly in the range of a few tens of ohms. As far as strained CNTs, Paulson et al reported [6] that using an atomic force microscope probe, they found that in some samples, changes in the contact resistance dominated the measured resistance change; while in other experiments, strain that was large enough to fracture the tube could be applied without significantly changing the contact resistance.

2. Experimental details

2.1 Growth of vertically aligned carbon nanotube arrays

A layer of titanium was coated onto a piece of quartz plate by using electron beam evaporation technique. Before the sputtering of iron catalyst thin film, a thin layer of silicon was sputtered onto the titanium layer in order to prevent the iron catalyst from defusing into titanium. Silicon and iron thin film sputtering processes were carried out in a RF magnetron sputtering system with a two-inch magnetron sputtering gun. The sputtering chamber was evacuated to a pressure lower than 1×10^{-6} torr. Argon gas was introduced into the sputtering chamber with a flow rate of 64 sccm. RF power was fed

into the gun through a matching network to generate a plasma. During sputtering, the vacuum pressure in the chamber was kept 20 mtorr.

After the deposition of iron catalyst film onto the substrate, the sample was oxidized in air at 300°C for 8 hours. Thermal CVD of carbon nanotubes was performed in a vacuum furnace filled with a gas mixture of acetylene and argon at a pressure of 70 torr. The flow rates for argon and acetylene were 75 sccm and 20 sccm, respectively. Before the gas mixture was fed into the furnace, the substrate was heated to 700°C in vacuum and the temperature was remained constant during the 20 minutes growth of carbon nanotubes. Vertically aligned carbon nanotubes grew on the substrate with a uniform length about 60 μm. Shown in Figure 1 is a SEM photograph of a vertically aligned carbon nanotube coating on titanium/silicon coated quartz.

2.2 Characterization of moving contacts of carbon nanotubes to metal electrodes

An inch-worm with nano-meter linear resolution was used to control the position of a gold wire of 25 μm in diameter that was perpendicular to the substrate on which vertically aligned carbon nanotubes were grown. The gold wire was, in some experiments, made into a small loop so that the gold wire was in parallel with the substrate when it was in contact with the vertically aligned carbon nanotubes. A 60 Hz AC voltage was applied through a current limiting resistor between the gold wire and a piece of gold foil, which formed a low-resistance contact to the carbon nanotube coatings. A multi-channel oscilloscope was applied to view the waveforms of the contact potential, conducting current, and the applied voltage. Contact resistance was calculated by dividing the contact potential by the current flowing through the contact. A

schematic diagram showing the experimental apparatus for the measurements is shown in Figure 2.

3. Results and discussion

3.1 Gold wire of 25 μm in diameter moving perpendicularly to the substrate in parallel with vertically aligned carbon nanotubes

A current limiting resistor of 5 kΩ was connected in series with the metal-carbon nanotube contact and a 60Hz power supply was used to apply a 10 volts peak-to-peak sinusoidal voltage across the current limiting resistor and the contact. Typical waveforms for the voltage across the contact and that for the voltages across the current limiting resistor are shown in Figure 3. The voltage across the current limiting resistor divided by the resistance equals to the current flowing through the contact.

Shown in Figure 4-6 are the contact potential, conducting current, and contact resistance of a gold wire that was inserted into a vertically aligned carbon nanotube coating in a direction with the gold wire being in parallel with carbon nanotubes and perpendicular to the substrate.

When the gold wire was moved closer to the carbon nanotube and eventually brought in contact with some of the carbon nanotubes, the voltage across the contact (see Figure 4 (triangle shaped curve)) decreased rapidly from five volts to less than one volt within a very short distance of one or few micrometers. Further insertion of the gold wire into the carbon nanotube array led the contact potential to decrease to about 0.2 Volts. While the contact potential decreased, the conducting current (see Figure 5 (triangle shaped curve)) increased from zero to 1000 μA, which was limited by the power supply voltage and the

current limiting resistor. The contact resistance (see Figure 6 (triangle shaped curve)) decreased from more than 3 kΩ to about 200 Ω.

When the gold wire was pulled out from the carbon nanotube array, the conducting current remained at 1000 μA and the contact potential and contact resistance remained low until the tip of the gold wire was pulled out up to a position higher than the top of the carbon nanotube array as shown in Figure 4 (square shaped curve). When the gold wire was further pulled away from the substrate, the contact potential and the contact resistance increased with simultaneously decreasing of the conduction current decreased. The contact resistance rose to around 5 kΩ at a position where the tip of the gold wire was above the top of the carbon nanotube array by about 35 μm. The contact resistance then jumped to infinity. During this period of measurements, carbon nanotubes attached to the gold wire were forming electrical contact with the carbon nanotubes grown on the substrate surface. The conducting path disappeared either when the carbon nanotubes attached to the gold wire broke or the attached carbon nanotubes were completely pulled away and out of the carbon nanotube array causing the contact to become an open circuit.

To test the effect of current load on contact resistance, the applied voltage was increased from 10 volts peak-to- to 40 volts peak-to-peak with other parameters kept the same. The gold wire left inserted into the aligned carbon nanotube was first pulled out gradually while the contact resistance was measured. The gold wire was pulled away from the substrate until the conducting path disappeared and the current became zero. The gold wire was then pushed towards the substrate into the aligned carbon nanotube. The gold wire was later pulled away from the substrate again. The contract resistance as a function of the relative position of the tip of the gold wire to the top surface of the

carbon nanotube coating is shown in Figure 7. The contact resistance is about the same as that measured using a 10 volt peak-to-peak power supply. However, the low-current and high-resistance tails that show in Figure 6 do not show up in Figure 7. It is probably because that the higher current level and higher open circuit voltage across the contact made the high contact resistance state, where carbon nanotubes attached to the gold wire contacted carbon nanotubes grown on the substrate, unstable and disconnected the circuit.

3.2 A loop of about 1mm in diameter made of gold wire of 25 μm in diameter moving towards or away from the substrate

Shown in Figure 8-10 are the contact potential, conducting current, and contact resistance between a loop of about 1 mm in diameter made of a gold wire of 25 μm in diameter, which was inserted into and made contact with a vertically aligned carbon nanotube coating, and the aligned CNTs. The gold wire that made the loop was in a direction perpendicular to the aligned carbon nanotubes and in parallel with the surface of the substrate when it was moved towards or away from the substrate. A current limiting resistor of 5 kΩ was connected in series with the metal-carbon nanotube contact and a 60Hz power supply was used to apply a 10 volts peak-to-peak sinusoidal voltage across the current limiting resistor and the contact.

When the gold loop was moved close to the carbon nanotube coating and eventually brought in contact with some of the carbon nanotubes, the voltage across the contact (see Figure 8 (triangle shaped curve)) decreased first rapidly from five volts to three volts within a very short distance of travel by one or few micrometers. Further insertion of the gold loop into the aligned carbon nanotubes led the contact potential to gradually decrease to about 0.4 Volts. While the contact potential decreased, the conducting

current (see Figure 9 (triangle shaped curve)) increased from zero to 400 μA rapidly and then gradually increased to 1000 μA, which was the maximum value limited by the power supply voltage and the current limiting resistor. The contact resistance (see Figure 10 (triangle shaped curve)) decreased from more than 7 kΩ to about 400 Ω.

When the gold loop was pulled away from the aligned carbon nanotubes near the top surface of the aligned carbon nanotubes coating, the conducting current decreases gradually from 1000 μA while the contact potential increased to five volts and the contact resistance increased to around 8 kΩ. The contact resistance then jumped to infinity when an open circuit was formed. When the gold loop was pulled away from the aligned carbon nanotubes, which were oriented perpendicularly to the gold wire, carbon nanotubes did not seem to attach to the gold wire very well. The continuous conductivity after the gold wire was pulled above the top of the surface of aligned carbon nanotube coating, which was observed when a gold wire was inserted and then pulled out of aligned carbon nanotubes as described in the previous section, was not observed in the case of a gold loop. With carbon nanotubes aligned vertically and contacted with the gold wire at about ninety degrees, the contact area between a carbon nanotube and the gold wire was smaller than that between a carbon nanotube and a gold wire aligned in parallel with respect to each other. Varying of the orientation of the gold wire with respect to the aligned carbon nanotubes caused the differences in the contact resistance and the capability for carbon nanotubes to attach to the gold wire and get pulled apart from the substrate when the gold wire or loop moved away from the substrate.

3.3 Applications of a moving electrical contact between a metal electrode and vertically aligned carbon nanotubes

Electrical contacts made of nanotubes and metal counter-electrodes may find applications where nano-meter sized electrical interconnects are needed for coupling electrical current and potential between two moving micro-devices. For example, carbon nanotubes can be selectively grown in a pre-designed pattern in desired areas on a planar or non-planar substrate, which is made into micro-systems such as micro-electro-mechanical systems (MEMS).

The rapid change of contact potential and contact resistance with respect to the relative position and orientation of a gold wire may be applicable as a sensor. When a micro-meter sized gold wire is attached to a cantilever which responds to acceleration, pressure, or temperature, a small move of the gold wire against a vertically aligned carbon nanotube coating will cause a large change in the voltage across the contact between the gold wire and the carbon nanotube coating as well as the contact resistance. This change will serve as the output of an accelerometer, a pressure sensor, or a temperature sensor.

4. Conclusions

Electrical characteristics of contacts between a gold wire and vertically aligned carbon nanotube coatings are reported and discussed. Contact resistances ranging from 200 Ω to several thousands of ohms have been measured when a gold wire of 25 μm in diameter was brought in contact with vertically aligned carbon nanotube coatings. The gold wire was allowed to move with respect to the carbon nanotube coating. If constant contact resistance and contact potential are desirable, the relative position of the gold wire with respect to the top surface of the carbon nanotube coating needs to be kept the same. A strong adhesion of carbon nanotubes to the substrate, a low adhesive force between

carbon nanotubes and the moving electrode, and a low coefficient of friction are also desirable for novel applications of carbon nanotubes as an electrical contacting material between two moving parts or devices. The change of the contact potential or contact resistance can be applied as a sensing signal to detect the displacement of a gold wire electrode with respect to a vertically aligned carbon nanotube coating. Further studies are being carried out to explore and optimize properties and applications of aligned carbon nanotubes as electrical contacts for moving parts and sensing elements.

Reference

[1] J. Hone, M.C. Llaguno, N.M. Nemes, and A.T. Johnson, J.E. Fischer, D.A. Walters, M.J. Casavant, J. Schmidt, and R.E. Smalley, "Electrical and thermal transport properties of magnetically aligned single wall carbon nanotube films," Appl. Phys. Lett. 77(5), 2000, 666-668

[2] P.J. de Pablo, E. Graugnard, B. Walsh, R.P. Andres, S. Datta, and R. Reifenberger, "A simple, reliable technigue for making electrical contact to multiwalled carbon nanotubes," Appl. Phys. Lett. 74(2), 1999, 323-325.

[3] B.Q. Wei, R. Vajtai, and P.M. Ajayan, "Reliability and current carrying capacity of carbon nanotubes," Appl. Phys. Lett. 79(8), 2001, 1172-1174.

[4] J. Tersoff, "Contact resistance of carbon nanotubes," Appl. Phys. Lett. 74(15), 1999, 2122-2124.

[5] A. Bachtold, M. Henny, C. Terrier, C. Strunk, and C. Schonenberger, J-P. Salvetat, J.-M. Bonard, and L. Forro, "Contacting carbon nanotubes selectively with low-ohmic contacts for four-probe electric measurements," Appl. Phys. Lett. 73(2), 1998, 274-276.

[6] S. Paulson, M.R. Falvo, N. Snider, A. helser, T. Hudson, A. Seeger, R.M. Taylor, R. Superfine and S. Washburn, "In-situ resistance measurements of strained carbon nanotubes," Appl. Phys. Lett. 75(19), 1999, 2936-2938.

[7] B. Wei, R. Spolenak, P. Kohler-Redlich, M. Ruhle, and E. Arzt, "Electrical transport in pure and boron-doped carbon nanotubes," Appl. Phys. Lett. 74(21), 1999, 3149-3151.

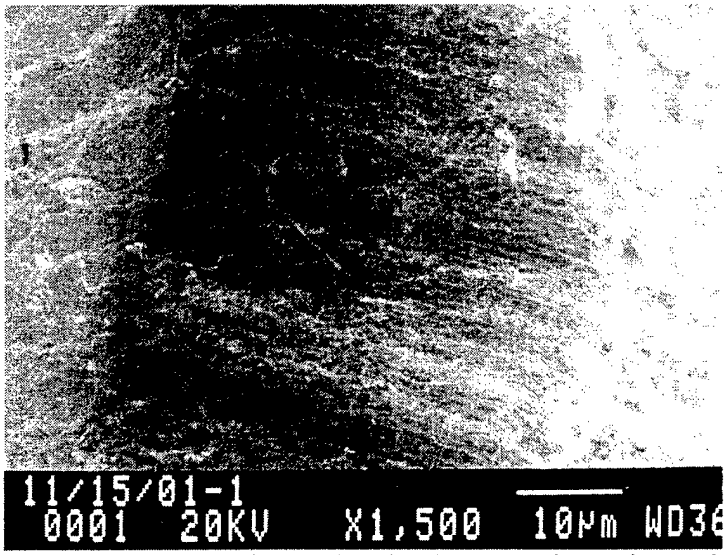

Fig.1. A SEM Photograph of a typical vertically aligned carbon nanotube coating used for this experiment.

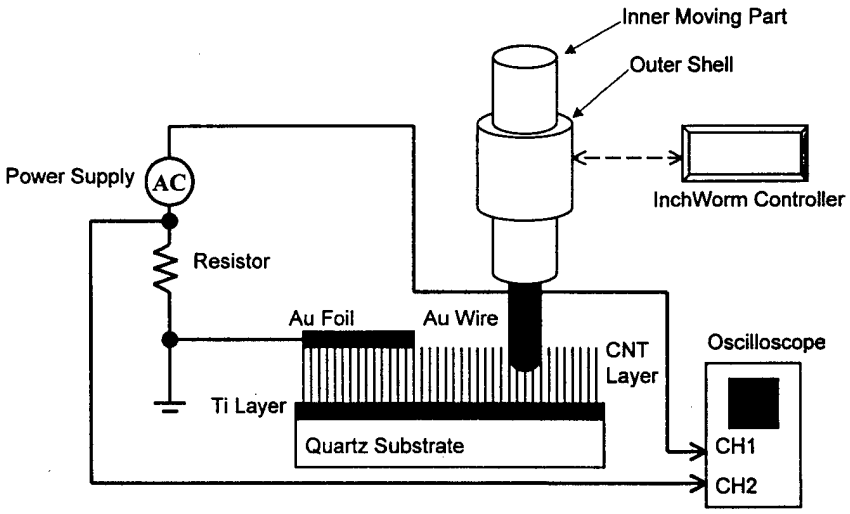

Fig.2. Schematic diagram of the electrical measurement setup.

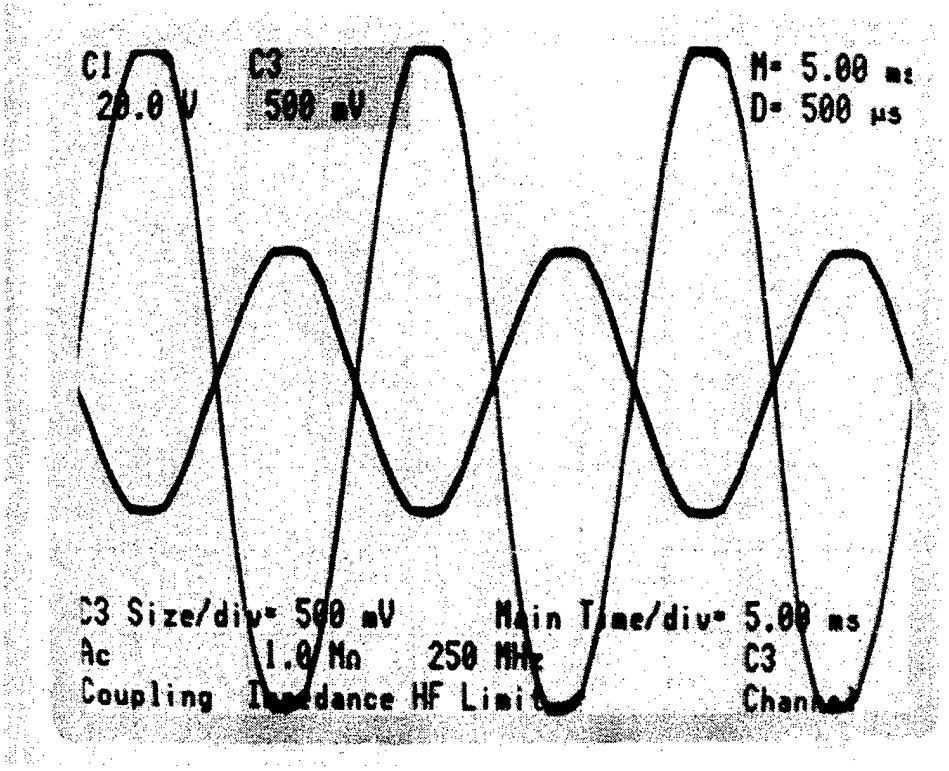
C1
20.0 V
C3
500 mV
M= 5.00 ms
D= 500 µs
C3 Size/div= 500 mV
Main Time/div= 5.00 ms
Ac
1.0 MΩ
250 MHz
C3
Coupling
Impedance
HF Limit
Channel

Fig. 3a

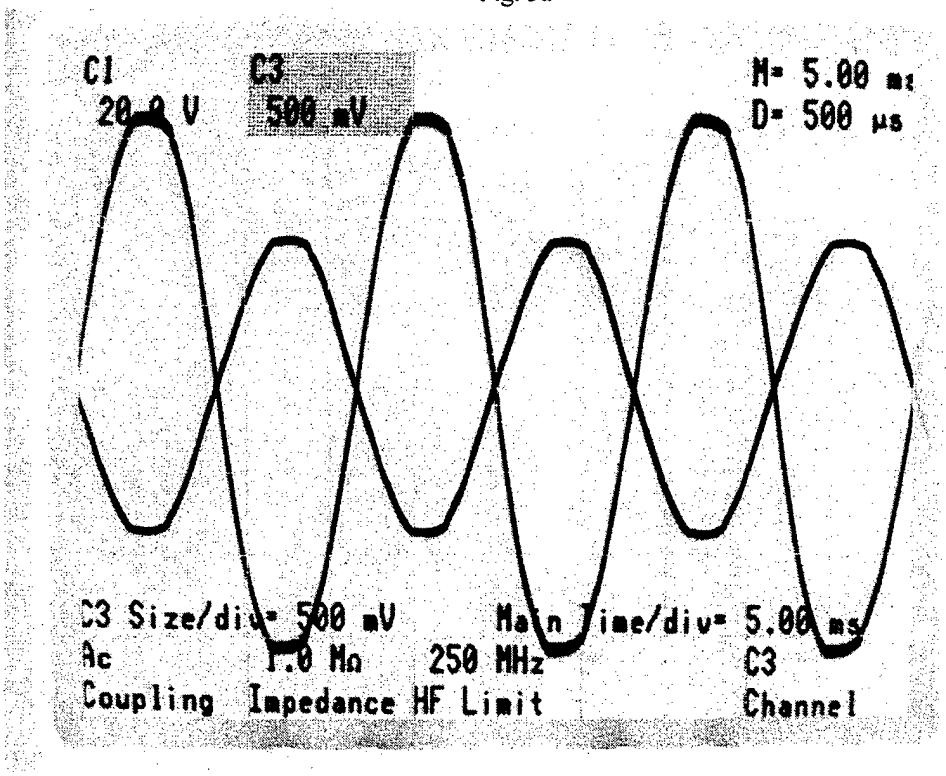
C1
C3
500 mV
M= 5.00 ms
D= 500 µs
C3 Size/div= 500 mV
Main Time/div= 5.00 ms
Ac
1.0 MΩ
250 MHz
C3
Coupling
Impedance
HF Limit
Channel

Fig.3b

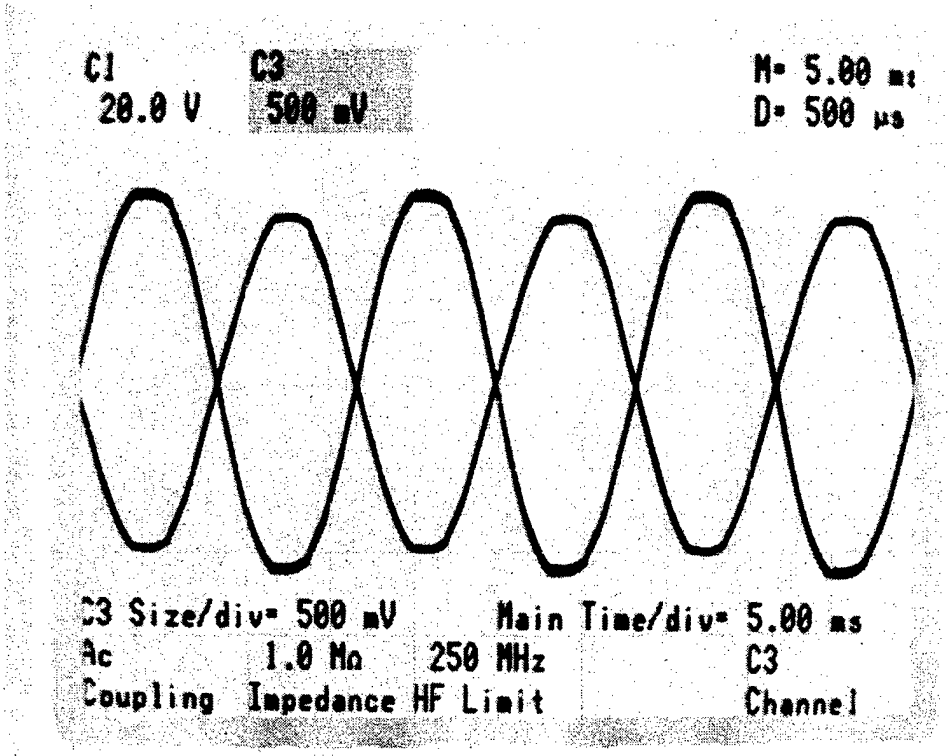

Fig.3c

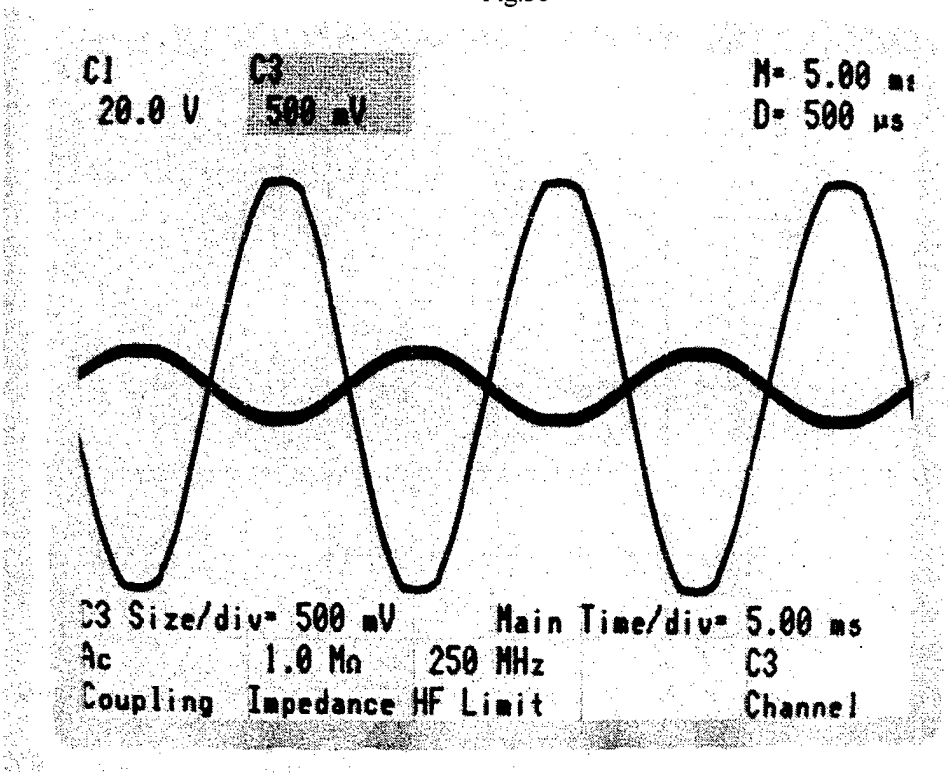

Fig.3d

Selected oscilloscope traces of contact voltages and conducting currents corresponding to four different positions of the gold wire with respect to the substrate.

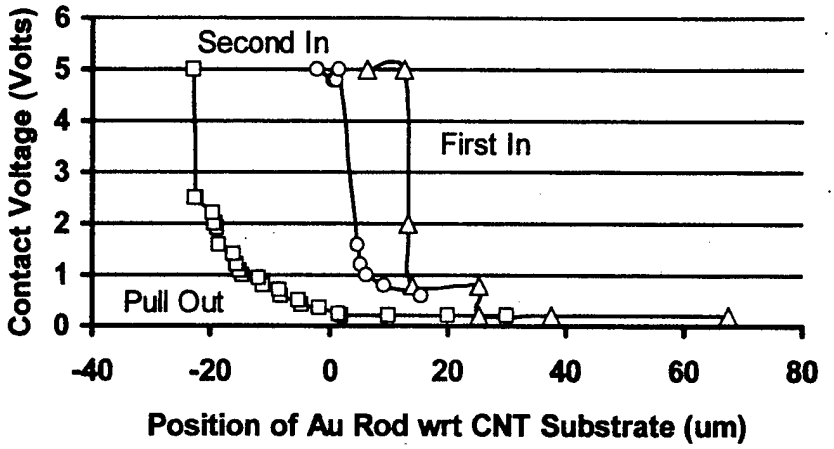

Fig. 4. Contact voltage across the gold wire and the vertically aligned carbon nanotube coating.

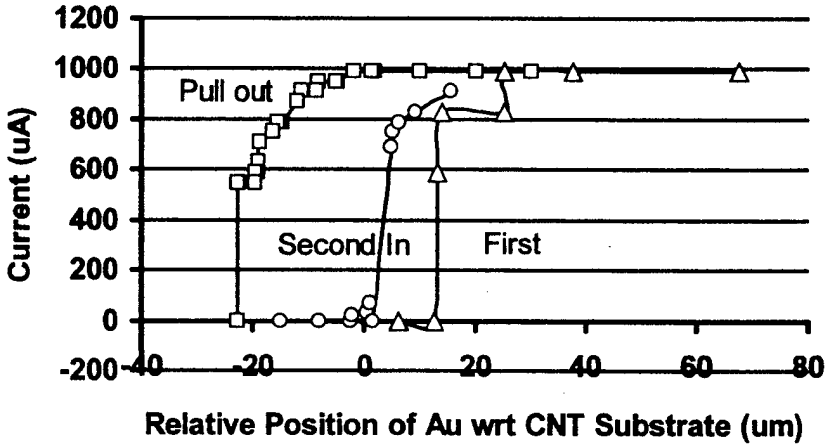

Fig. 5. Conduction current flowing through the contact between the gold wire and the vertically aligned carbon nanotube coating.

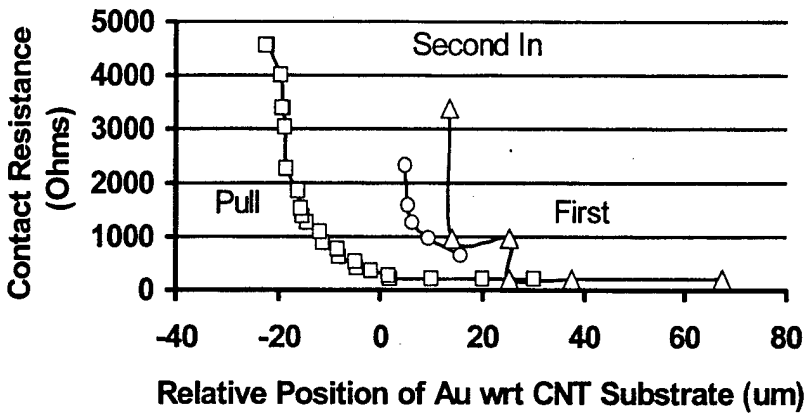

Fig. 6. Contact resistance between a gold wire and a vertically aligned carbon nanotube coating.

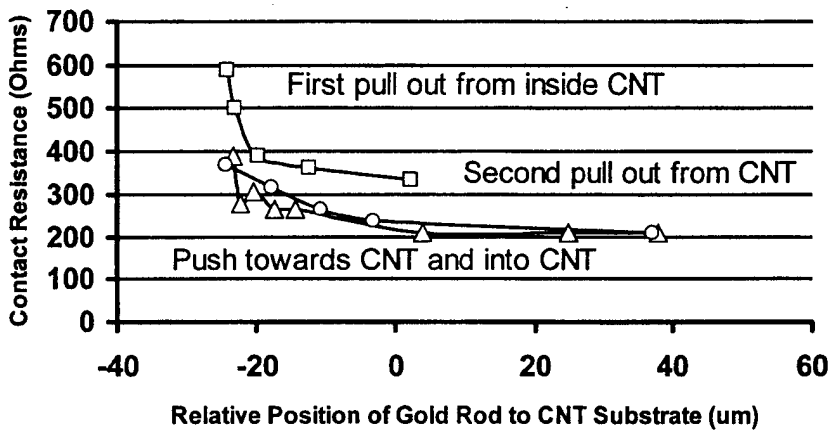

Fig. 7. Contact resistance between a gold wire and a vertically aligned carbon nanotube coating with current load equal to four times of that shown in Figure 6.

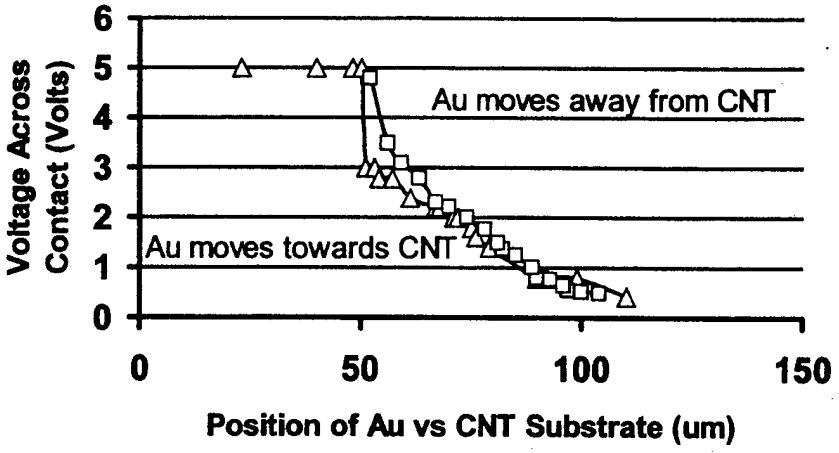

Fig. 8. Contact voltage across the gold loop and the vertically aligned carbon nanotube coating.

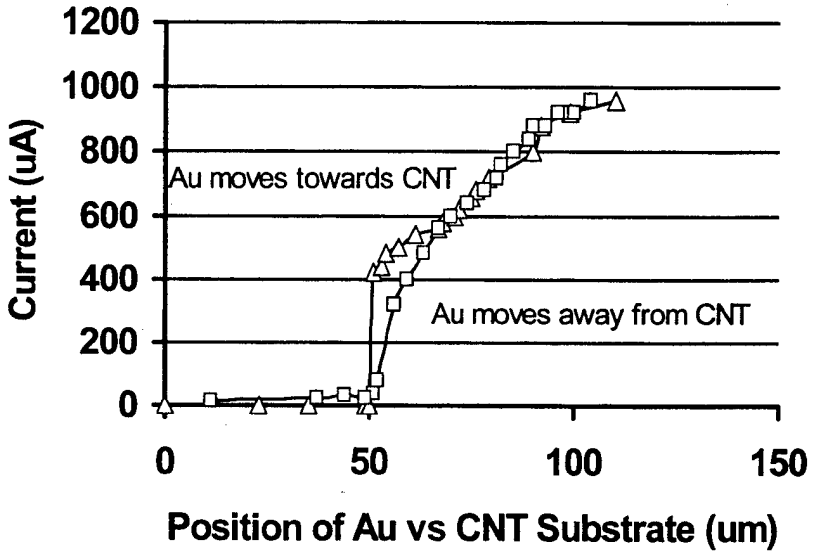

Fig.9. Conduction current flowing through the contact between the gold loop and the vertically aligned carbon nanotube coating.

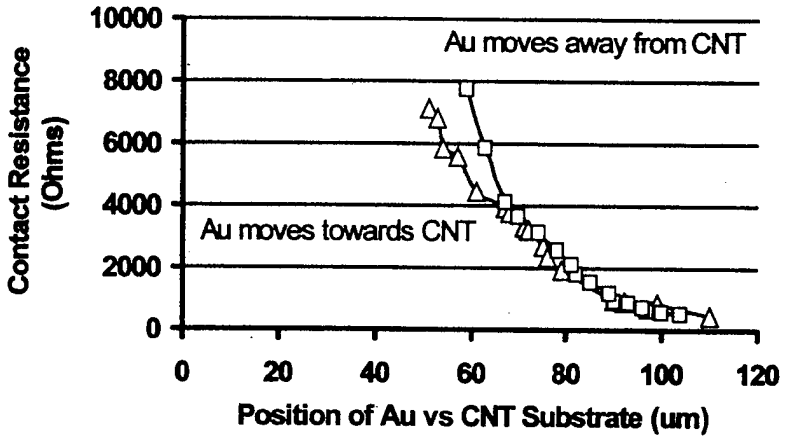

Fig.10. Contact resistance between a gold loop and a vertically aligned carbon nanotube coating.

Presented in ICNDST-8 and submitted to Diamond and Related Materials

Microwave Plasma CVD of Diamond and Nanodiamond Coatings In Vapor Mixtures of Methanol and Ethanol and Applications to Cold Cathodes

Chao. Liu and Yonhua Tzeng

Department of Electrical and Computer Engineering

Auburn University, Auburn, Alabama 36849 (USA)

Atsushi Hirata

Department of Mechanical Sciences and Engineering

Tokyo Institute of Technology, Tokyo 152-8552, Japan

Abstract

Diamond and nanodiamond coatings were deposited on molybdenum by means of microwave plasma enhanced chemical vapor deposition in vapor mixtures that were fed into a CVD reactor from premixed liquid solutions of methanol and ethanol through a needle valve without the use of hydrogen carrier gas or any other gaseous additives. Molybdenum electrodes after being coated with diamond or nanodiamond showed electron field emission characteristics that depended on the grain size, whether the coating was a continuous film or discrete particles, and the inclusion of non-diamond contents in the coating. Continuous diamond films of high quality required the highest electric field among all specimens for the on-set of cold electron field emission compared to discrete diamond particles and nanodiamond films with high-non-diamond contents. Nanodiamond coatings deposited in methanol-ethanol vapor mixtures at elevated

substrate temperatures allowed cold electron field emission at a much lower electric field than that required for high quality and well faceted diamonds. The turn-on electric field for field emission of electrons from optimized nanodiamond coatings was measured to be between one and two volts per micrometer.

* Corresponding author's e-mail address: tzengy@eng.auburn.edu

Keywords: CVD, diamond, field emission, plasma

1. Introduction

Carbon coatings, for example, diamond, diamond like carbon, graphite, and carbon nanotubes, have been studied extensively for applications to cold-cathode electron field emitters that desire cold electron emission at high current densities and at low electric fields [1-5]. The voltage needed for electron emission from a cold cathode that is placed at a fixed distance from the anode is lower when the surface of the cathode has a lower positive electron affinity or preferably a negative electron affinity (NEA) and/or when the field enhancement factor at the electron emission sites is higher.

Diamond (111) surface with hydrogen termination has been reported to exhibit negative electron affinity and is considered as one of the promising cold cathode materials for applications which require electron field emission at low electric fields, and excellent chemical and physical stability [1]. However, a cold undoped diamond of high purity is an electrical insulator that severely restricts the current density of electron emission while the hydrogen termination on the diamond surface tends to be altered by the electron emission process as well as ion bombardment to the diamond surface.

Carbon nanotube is an excellent example that exhibits a very large field enhancement factor favorable for cold cathode electron emission at a low applied electric field, which

is the applied voltage divided by the distance between the cathode and the anode. Although the work function of carbon nanotube is not low, the aspect ratio, which is the ratio of the effective length of a carbon nanotube to the effective radius of curvature of the tip of the carbon nanotube, is very high. High aspect ratio makes the local electric field near the tip of a carbon nanotube hundreds of even thousands of times higher than the electric field calculated by dividing the applied voltage by the distance between the cathode and the anode. Some adsorbates at the tip of a carbon nanotube may also lead to even easier cold electron emission assisted by tunneling mechanisms [6].

Besides high purity diamonds with NEA and carbon nanotubes with high field enhancement factors, many carbon coatings have been reported to exhibit good or excellent cold electron field emission characteristics by means of optimized control of the nanostructures of the carbon coatings as well as the contents of sp^2 versus sp^3 and non-carbon elements in the coatings [7-12].

Recent efforts in diamond film synthesis aiming at electron field emitters with low turn-on electric fields as well as high emission current densities are focused mainly on (i) the fabrication of diamond films with morphology or shapes which give local electric field enhancements [13-14], (ii) surface modification of diamond films to achieve a negative electron affinity, or at least a low positive electron affinity [15-16], (iii) inducing defects into the bulk of diamond or onto the surface of diamond films to help with electron injection through the diamond film and from the surface of diamond into vacuum [17-18], and (iv) varying the content of sp^2 in the diamond film in order to generate conductive path for electrons, or to form "internal" field enhancement in the diamond film [19-20].

Diamond, nanodiamond, and diamond-like carbon films have been deposited by means of chemical vapor deposition (CVD) assisted by various energy sources in addition to thermal excitation. DC, RF, and microwave plasmas as well as laser illumination have all been demonstrated to be effective in creating suitable chemical, physical conditions for diamond, nanodiamond, and diamond-like carbon deposition. Methane, among other hydrocarbons, and organic solvents, is the most commonly used carbon source for the growth process while hydrogen gas is usually the major feedstock for carbon chemical vapor deposition that aims at achieving high crystalline quality of diamond [2][5][21].

Most diamond CVD processes involve the use of hydrogen or some gaseous feedstock that is stored as a compressed gas at ambient temperature. We reported a diamond CVD process using a methanol pre-mixed liquid solution alone without intentionally added water as the feedstock for the deposition of high-quality diamond films [22-23]. In the paper, results will be presented from the methanol based CVD process that has been altered in order to deposit diamond and diamond-like carbon coatings ranging from diamond to highly graphitic carbon coatings for the purpose of achieving a high-performance cold cathode electron emitter. Scanning electron microscopy and Raman spectroscopy were used to correlate the morphology and crystalline quality of the CVD diamond and diamond-like films with electron field emission characteristics.

2. Experimental details

CVD process was carried out by the assistance of a microwave plasma in a vapor mixture of methanol and ethanol. The ratio, by weight, of methanol to ethanol, the microwave power, the vapor pressure, and the substrate temperature were varied in order to deposit carbon coatings ranging from high-quality diamond crystals and films to nanodiamonds as well as highly graphitic carbon deposits.

A dual color optical pyrometer was used to measure the substrate temperature as well as determine the termination time for the deposition process in order to obtain a coating with either discrete particles or a continuous film. The interference between the incident light and the reflected light through the growing carbon deposits from the substrate results in the dual color optical pyrometer reading oscillating in time. The oscillating readout started when deposits are still in the form of discrete particles or an incomplete film with many voids before a continuous carbon film is finally formed. Adjusting the growth time by counting the number of cycles or a fraction of a cycle of the oscillation of the dual-color pyrometer readout, diamond or nanodiamond coatings in the form of either discrete particles or a continuous film of pre-determined thickness were obtained. Figure 1 shows a typical pyrometer readout plotting recorded by a chart plotter.

The effect of C/O ratio in the feedstock was studied by varying the ratio of methanol to ethanol in the pre-mixed liquid solution used as the feedstock for carbon deposition. Power density of the microwave plasma was varied and used to deposit carbon coatings at elevated substrate temperatures. Two-step nucleation and growth processes were also applied to first achieve high nucleation density by a lower power-density microwave plasma followed by a higher power-density microwave plasma at a higher vapor pressure

for altering the crystalline properties and graphitic/diamond contents of the deposited carbon coatings.

Polished molybdenum plates were used as the substrates and were put onto a water-cooled substrate holder after having been seeded with diamond by rubbing the substrates with diamond paste. The substrate temperature was monitored by a dual color optical pyrometer with its readout being plotted using a chart recorder.

Microwave plasma CVD diamond and diamond-like films were investigated by scanning electron microscopy and Raman spectroscopy.

Raman spectroscopy is a powerful method in the examination of synthetic carbon coatings. It can characterize not only the quality of the deposited carbon films, but the contents of various carbon phases quantitatively. In case of CVD diamond, a number of Raman features can be used to investigate the deposited carbon films. The full width at half maximum (FWHM) at 1332 cm^{-1} reveals the impurity level and crystalline quality of a diamond [24-26]. The intensities of the sp^2-bonded carbon bands can also be compared to that of the diamond peak. Typical sp^2-bonded bands include (i) 1580 cm^{-1}, which is the signature of crystalline graphite; (ii) 1550 cm^{-1}, which is referred as 'G' band; (iii) 1350 cm^{-1}, which is the signature of microcrystalline graphite and also referred as 'D' band stands for 'distorted band'; and (iv) 1450-1500 cm^{-1}, which is considered as signal for amorphous carbon [25]. In this paper, an argon laser source was used to illuminate perpendicularly the carbon films. Raman spectra from 880 cm^{-1} to 1840 cm^{-1} were recorded.

Electron field emission measurements were carried out in a high-vacuum chamber pumped to the order of 10^{-7} torr. Diamond samples were put into the chamber against a

flat counter-electrode. The distance between the anode and cathode was kept by an electrically insulating spacer, such as a glass cover sheet, with a known thickness. A DC power supply was used to apply electric field between the electrodes. The electron emission current was measured by a pico-ammeter and recorded using a computer, which controlled both the power supply and the ammeter. Correlations among CVD conditions, characteristics of the deposits, and electron field emission performance were obtained and analyzed.

3. Results and discussion

The effects of C/O ratio on the characteristics of carbon deposits and electron field emission were studied by selecting microwave power and vapor pressure so as to keep the substrate temperature around 800°C while varying the ratio of methanol to ethanol by weight in the pre-mixture liquid feedstock. Figure 2 shows the SEM photographs for carbon coatings obtained with the ratio of methanol to ethanol by weight being 100:0 or 100:30. The growth time was two hours. Figure 3 and Figure 4 show the Raman spectra and the electron field emission current-electric field (I-E) plots for samples corresponding to the ratio, by weight, of methanol to ethanol of (a) 100:0, (b) 100:5, (c) 100:30, and (d) 0:100, respectively. The growth time was two hours for (a) to (c) and 30 minutes for (d).

For the aforementioned growth time, SEM photographs indicate that the growth rate of the carbon coating increases with increasing ethanol concentration in the methanol based feedstock. Coatings deposited without adding ethanol, that is, with a 100% methanol plasma, contain discrete particles instead of continuous films. The diamond film deposited in the plasma with a ratio, by weight, of methanol to ethanol being 100:30 shows a continuous coating. The carbon coating obtained with methanol-to-ethanol ratio

of 100:30 exhibits the best electron emission behavior, among all carbon coatings deposited at around 800°C in terms of a low on-set electric field and a high electron emission current density.

A sharp diamond peak at around 1330 cm^{-1} is observed in the Raman spectrum for the diamond deposits obtained from 100% methanol feedstock. A broad band around 1520 cm^{-1} is also observed. This feature is a demonstration of sp^2 clusters [27], and can be considered the mixture of the Raman band of nanocrystalline sp^2 content, which is a doublet near 1500 cm^{-1} [28], and the downshifting of crystalline graphite G band from 1550 cm^{-1} to 1525-1528 cm^{-1} [29]. With increasing ethanol concentration, the diamond peak becomes less intensive while the intensity of sp^2-bonded broad band increases in intensity and the diamond peak is not detectable when the methanol to ethanol ratio is 0:100.

A wide and low-intensity band around 1140 cm^{-1}, which resulted from small grain-size (<5 nm) a-diamond [19], can also be found in some of the spectra. By applying the nanocrystalline diamond model proposed by Obraztsova et al. [19], the grain sizes of sample (a), (b) and (c) are in the range of micro-crystalline (>50 nm). The less intense diamond peak and the broadening of sp^2 band in the Raman spectra of sample (b) and (c) indicate that the grain sizes of sample (b) and (c) are smaller than that of sample (a). The Raman spectrum of sample (d) matches that of the CVD nanocrystalline diamond films, indicating that the grain size of diamond film deposited with 100% ethanol is less than 10 nm.

Among carbon coatings deposited at around 800°C, the coating shown in Figure 4(c) exhibits the best electron field emission behaviors in terms of a low onset electric field

and a high electron emission current density. The nanocrystalline diamond film shown in Figure 4(d), although having a high density of non-diamond contents and a large number of smaller grains and grain boundaries, did not exhibit any advantage in electron field emission over other specimens with larger gain sizes.

High substrate temperature is in favor of the growth of graphitic or non-diamond phases in the carbon coatings. In the following discussion, carbon coatings were obtained at elevated substrate temperatures by increasing the microwave power and vapor pressure. The experiments were carried out by first using a mixture of methanol and ethanol with a ratio, by weight, of 100:10 as the feedstock. The substrate temperature, which was measured by a dual-color optical pyrometer, was 1270°C. After 18 minutes of deposition, there was no carbon coating on the substrate. Because of the high oxygen content in the methanol/ethanol mixture, the etch rate of carbon by oxygen containing plasma at such a high temperature suppressed the nucleation and deposition of carbon on the substrate surface.

Thus, a two-step CVD process was carried out to obtain carbon deposition at elevated substrate temperatures in the environment of methanol and ethanol vapor mixtures. In the first step, microwave power and vapor pressure were selected to generate a plasma that heats the substrate to a temperature around 900°C in order to achieve nucleating and coating on the substrate with carbon deposits. Microwave power and vapor pressure were later increased to 1800 watt and 70 torr, respectively, to allow the carbon deposits to grow in size and thickness. In the second step, the substrate temperature was monitored by a dual-color optical pyrometer, and the growth time was controlled by counting the

cycles of oscillation of the pyrometer readouts. Typically the deposition was terminated after the pyrometer readouts had shown one and a half cycles of oscillation.

Figure 5 shows the SEM photographs for carbon coatings deposited by the two-step process. The methanol-to-ethanol ratio, by weight, was 100:10, 50:50, and 30:60, respectively. Figure 6 and Figure 7 show Raman spectra, and electron field emission I-E curves for carbon coatings deposited with methanol-to-ethanol ratio, by weight, being (a) 100:10, (b) 60:30, (c) 50:50, (d) 30:60, and (e) 0:100, respectively. The nucleation time/growth time, in minutes, was (a) 30/25, (b) 20/9, (c) 25/8, (d) 7/9, and (e) 14/7, respectively. The maximum substrate temperature measured during the nucleation step were about 900°C. The substrate temperature measured during the growth step was in the range of 1200-1400°C.

Additional experiments were carried out with the same two-step process using 100% methanol as the feedstock. There were no coatings after a relatively long nucleation step of 50 minutes. With a high concentration of oxygen in the plasma at an elevated substrate temperature, the etch rate of oxygen radicals for carbon deposits is too high for carbon deposition under these CVD conditions.

Among the measured electron field emission I-E characteristics, the carbon coatings obtained with the ratio of methanol to ethanol equal to 50:50 and 60:30 exhibit the best electron field emission behaviors in terms of the low onset electric field and the high emission current density. Electron field emission was somewhat less efficient from carbon coatings obtained with methanol to ethanol ratios of 30:60 and 0:100. The sample with methanol to ethanol ratios of 100:10 has the worst electron field emission characteristics.

The Raman spectrum for the carbon coating shown in Figure 6(a) includes a sharp diamond peak at 1334 cm^{-1}, indicating a large content of good quality diamond in the film. With increasing ethanol concentration in the liquid mixture, the diamond peak becomes wider and less intense (see sample 6 (b)) and finally disappears (see sample 6 (c) and 6 (d)). At the same time, the band with a maximum at around 1344-1347 cm^{-1} emerges while the intensity of the band near 1580 cm^{-1} increases. These two bands are believed to correspond to D band and graphite peak, respectively. This trend indicates that the deposited carbon coating becomes more graphitic as the ethanol concentration in the liquid mixture increases. The graphite peak at 1580 cm^{-1} becomes stronger and finally exceeds the D band as shown in the Raman spectrum of sample 6 (d), indicating that the carbon coating (sample 6 (d)) contains a high content of graphitic carbon.

Aforementioned results and discussion can be summarized as follows. Firstly, grain sizes of the carbon films deposited at elevated substrate temperatures are larger comparing with those of films deposited at lower temperatures as indicated by the disappearing of *a*-diamond band at 1140 cm^{-1}. Secondly, with increasing ethanol concentration, the volume ratio of sp^3-bonded contents to that of sp^2-bonded ones decreases as indicated by the widening of diamond peak as well as the increasing intensity of the sp^2-bonded bands. The O/C ratio decreases with increasing ethanol concentration in the liquid mixture and selective etching of sp^2 contents by oxygen radicals in the plasma becomes less effective.

4. Conclusions

At substrate temperatures around 800°C, CVD diamond and nanodiamond films with grain sizes ranging from tens of micrometer to tens of nanometer were deposited. The

higher the ethanol concentration was in the methanol/ethanol liquid mixture, the smaller the grain sizes of the deposited films were, and the higher concentration of sp^2-bonded contents the deposited films contained. Higher C/O ratio with increasing ethanol concentration made the oxygen concentration in the plasma lower with respect to carbon and the selective etching of sp^2-bonded contents in the deposited coating by oxygen radicals less effective. Electron field emission was not improved by making grain sizes smaller and concentration of sp^2 contents higher in the CVD carbon films deposited at around 800°C using mixtures of methanol and ethanol as the feedstock.

At elevated substrate temperatures above 1000°C, little nucleation of diamond and other carbons on the substrate occurred. A low temperature nucleation step was necessary before a higher temperature growth step. With increasing ethanol concentration in the liquid mixture, the deposited carbon films became increasingly graphitized. The electron field emission behaviors measured from the carbon coatings deposited at elevated temperatures are much better, in terms of low on-set electric field and high electron emission current density, than those from carbon films deposited at low temperatures. Although increasing the concentration of sp^2-bonded contents in carbon films deposited at low temperatures around 800°C did not improve significantly the electron field emission behaviors, carbon films that were deposited at elevated substrate temperatures and exhibited much better electron field emission behaviors did contain higher sp^2-bonded contents than those carbon films deposited at low temperatures.

References

[1] J. Robertson, Carbon 37 (1999) 759.

[2] W. Zhu, G. P. Kochanski, S. Jin, and L. Seibles, J. Vac. Sci. Technol. B 14(3) (1996) 2011.

[3] M. W. Geis, J. C. Twichell, and T. M. Lyszczarz, J. Vac. Sci. Technol. B 14(3) (1996) 2060.

[4] O. Groning, L-O. Nilsson, P. Groning, and L. Schlapbach, Solid-State Electronics 45 (2001) 929.

[5] V. I. Merkulov, D. H. Lowndes, L. R. Baylor, and S. Kang, Solid-State Electronics 45 (2001) 949.

[6] K.A. Dean, B. R. Chalamala, B. F. Coll, A. A. Talin, J. Trujillo, Y. Wei, and J. Jaskie, Proceedings of the Sixth Applied Diamond Conference/ Second Frontier Carbon Technology Joint Conference, NASA/CP-2001-210948, 2001, p. 708.

[7] I. Pavlovsky, R. L. Fink. L. F. Thuesen, Z. Yaniv, and R. Espinosa, Proceedings of the Sixth Applied Diamond Conference/ Second Frontier Carbon Technology Joint Conference, NASA/CP-2001-210948, 2001, p. 399.

[8] J. Krauser, A. Weidinger, M. Waiblinger, V. Hoffmann, C. Trautmann, B. Schultrich, H. Hofsass, and C. Ronning, Proceedings of the Sixth Applied Diamond Conference/ Second Frontier Carbon Technology Joint Conference, NASA/CP-2001-210948, 2001, p. 400.

[9] N. S. Xu, R. V. Latham, and Y. Tzeng, J. Phys. D: Applied Physics 26 (1993) 1776.

[10] N. S. Xu, R. V. Latham and Y. Tzeng, Electronics Letters 29(18) (1993).

[11] N. S. Xu, Y. Tzeng, and R. V. Latham, J. Phys. D: Appl. Phys. (Rapid Communication) 27 (1994) 1988.

[12] N. S. Xu, R. V. Latham and Y. Tzeng, Diamond Films and Technology 4 (4) (1994) 249.

[13] D. Hong and D. Aslam, IEEE Trans. Electron Devices, 45(4) (1998) 977.

[14] N. S. Xu, J. C. She, S. E. Huq, J. Chen, S. Z. Deng, and J. Chen, Ultramicroscopy 89 (2001) 111.

[15] I-Nan Lin, Y.-H. Chen, and H.-F. Cheng, Diamond and Related Materials 9 (2001) 1574.

[16] W. Zhu, C. Bower, G. P. Kochanski, and S. Jin, Solid-State Electronics 45 (2001) 921.

[17] Y. Show, T. Matsukawa, M. Iwase, and T. Izumi, Material Chemistry and Physics 72 (2001) 201.

[18] W. Zhu, G. P. Kochanski, S. Jin, and L. Seibles, J. Appl. Phys. 78(4) (1995) 2707.

[19] J. B. Cui, M. Stammler, J. Ristein, and L. Lay, J. Appl. Phys. 88(6) (2000) 3667.

[20] W. P. Kang, A. Wisitsora-at, J. L. Davidson, D. V. Kerns, Q. Li, J. F. Xu, and C. K. Kim, J. Vac. Sci. Technol. B 16(2) (1998) 684.

[21] N. Jiang, K. Sugimoto, K. Eguchi, T. Inaoka, Y. Shintani, H. Makita, A. Hatta, and A. Hiraki, Journal of Crystal Growth 222 (2001) 591.

[22] Y. Tzeng, Proceedings of ADC/FCT, August 31-September 4, 1999, Tsukuba, Japan, p. 420.

[23] Y. Tzeng, Proceedings of ADC/FCT, August 31-September 4, 1999, Tsukuba, Japan, p. 20.

[24] L. Robins, E. N. Farabaugh, and A. Feldman, J. Mater. Res. 5(11) (1996) 2456.

[25] C. Pickard, T. J. Davis, W. N. Wang, and J. W. Steeds, Diamond and Related Materials 7 (1998) 238.

[26] G. Morell, O. Quinones, Y. Diaz, I. M. Vargas, B. R. Weiner, and R. S. Katiyar, Diamond and Related Materials 7 (1998) 1029.

[27] M. Yoshikawa, Y. Mori, H. Obata, M. Maegawa, G. Katagiri, H. Ishida, and A. Ishitani, Appl. Phys. Lett.67 (5) (1995) 694.

[28] E. Obraztsova, K. G. Korotushenko, S. M. Pimenov, V. G. Ralchenko, A. A. Smolin, V. I. Konov, and E. N. Loubnin, NanoStructured Materials 6 (1995) 827.

[29] J. Shiao, R. W. Hoffman, Thin Solid Films 283 (1996) 145.

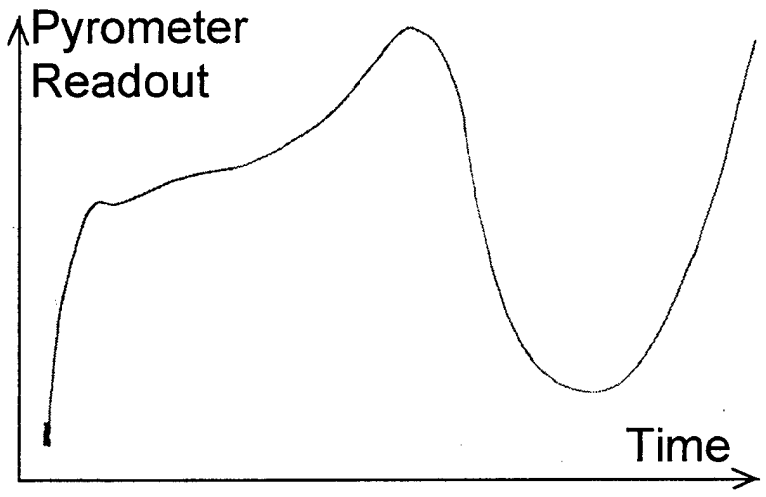

Fig. 1. An example of the optical pyrometer readout plotted by a chart recorder during a CVD diamond process. The readout oscillated for approximately one cycle in this example.

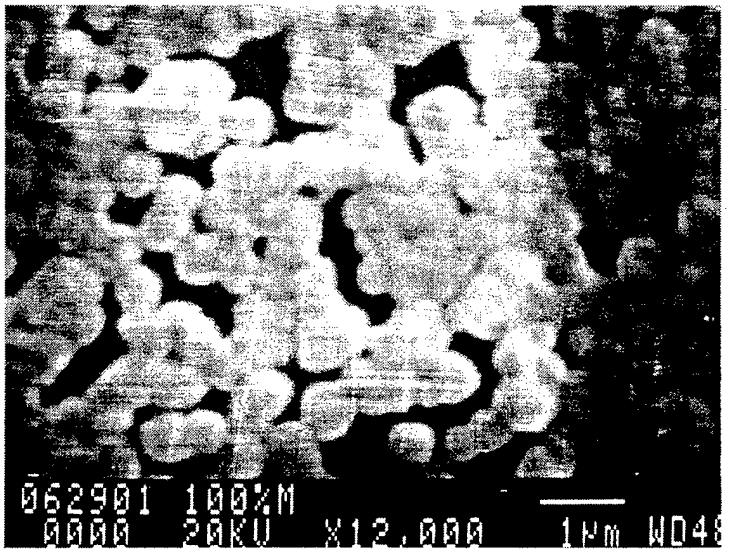

(a)

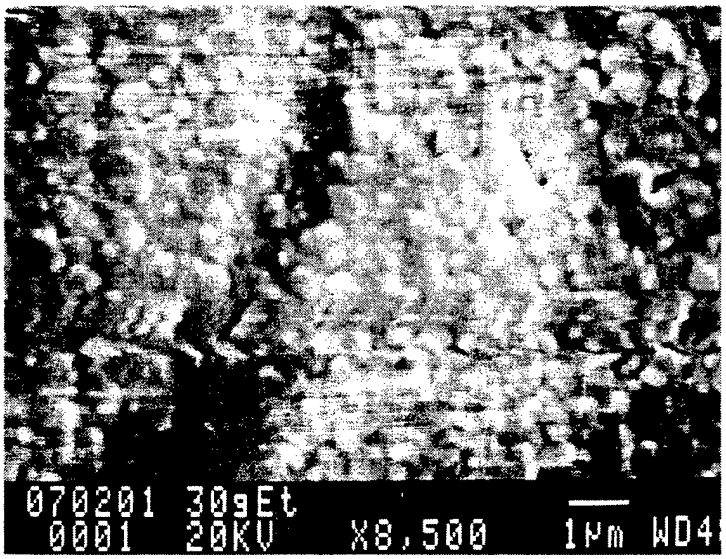

(b)

Fig. 2. Scanning electron microscopy photographs of CVD diamond samples deposited in microwave plasmas with methanol to ethanol ratio by weight of (a) 100:0 and (b) 100:30 at substrate temperature of 800°C. Growth time was 2 hours.

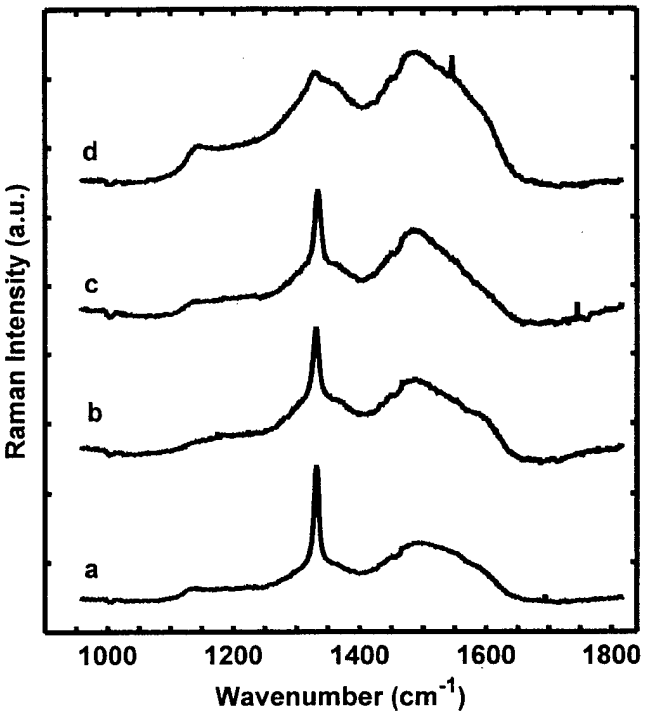

Fig. 3. Raman spectra of CVD diamond samples deposited in microwave plasmas with methanol to ethanol ratio by weight of (a) 100:0, (b) 100:5, (c) 100:30, and (d) 0:100 at substrate temperature of 800°C. Growth time were (a-c) 2 hours and (d) 30 minutes, respectively.

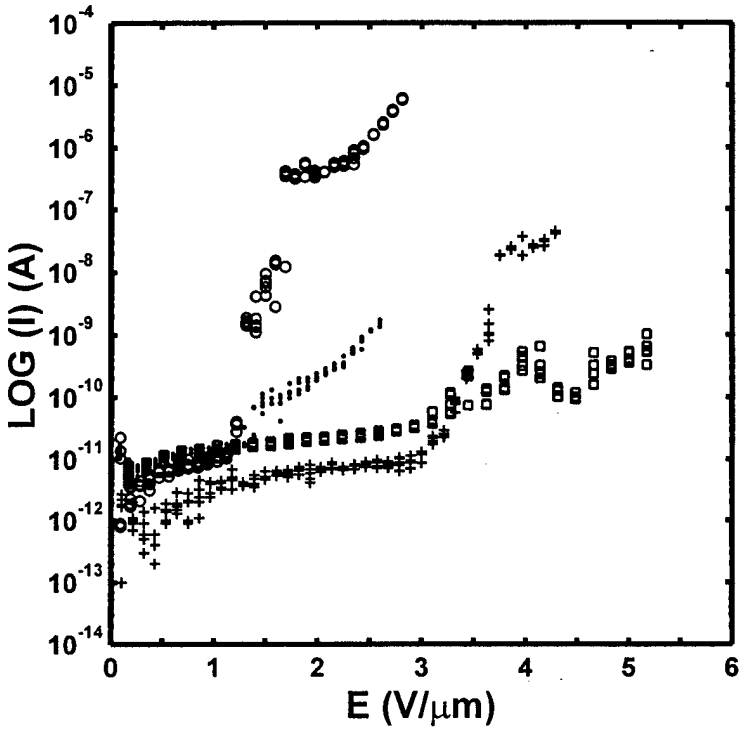

Fig. 4. Electron field emission I-E characteristics of CVD diamond samples deposited in microwave plasmas with methanol to ethanol ratio by weight of (a) 100:0 (dots), (b) 100:5 (squares), (c) 100:30 (circles), and (d) 0:100 (plus signs) at substrate temperature of 800°C. Growth times were (a-c) 2 hours and (d) 30 minutes, respectively.

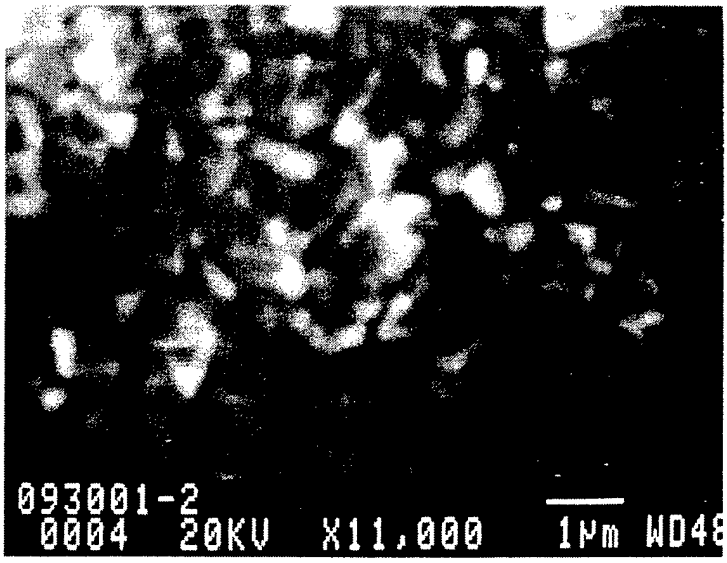
093001-2
0004 20KV X11,000 1µm WD4

(a)

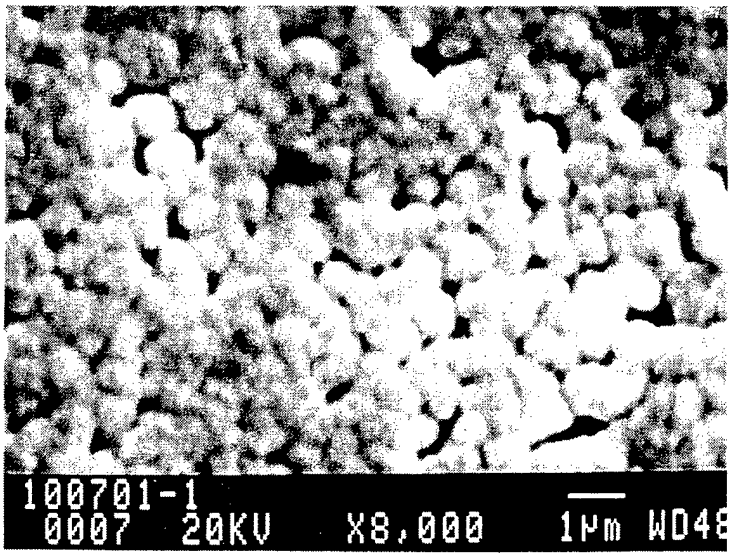
100701-1
0007 20KV X8,000 1µm WD4

(b)

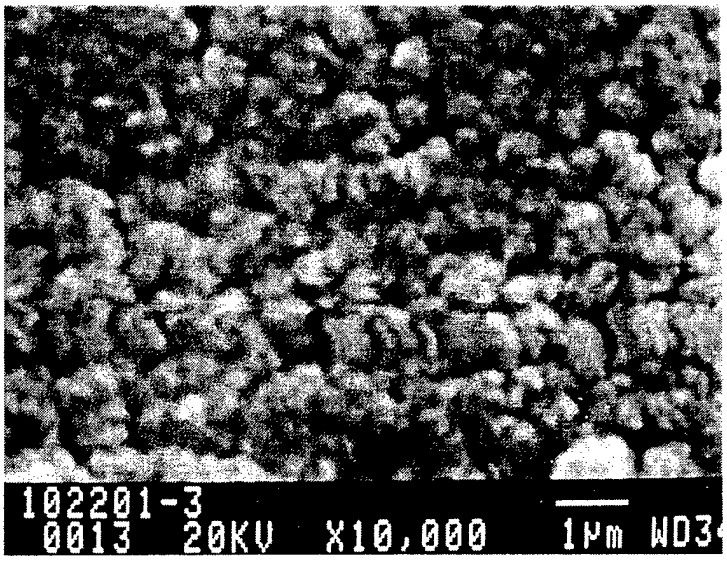

(c)

Fig. 5. Scanning electron microscopy photographs of CVD diamond samples deposited using a two-step process in microwave plasmas with methanol to ethanol ratio by weight of (a) 100:10, (b) 50:50, and (c) 30:60, respectively.

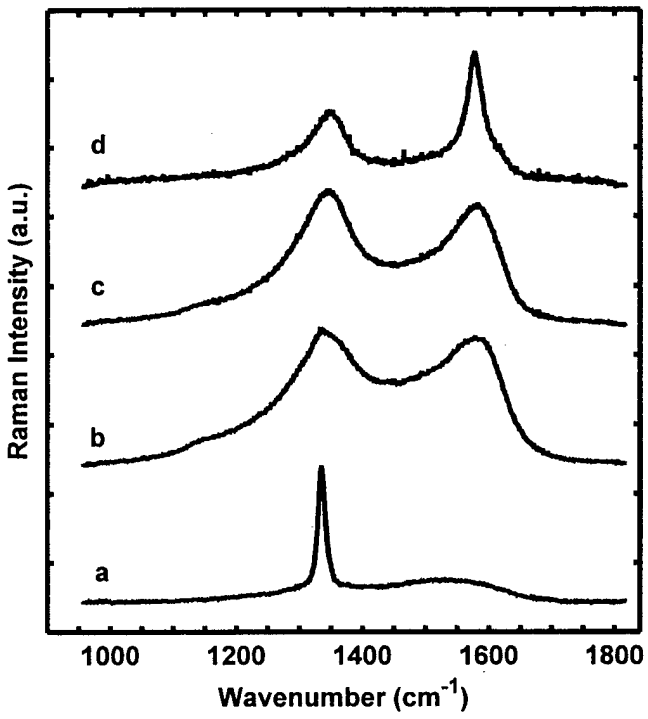

Fig. 6. Raman spectra of CVD diamond samples deposited using a two-step process in microwave plasmas with methanol to ethanol ratio by weight of (a) 100:10, (b) 60:30, (c) 30:60, and (d) 0:100, respectively.

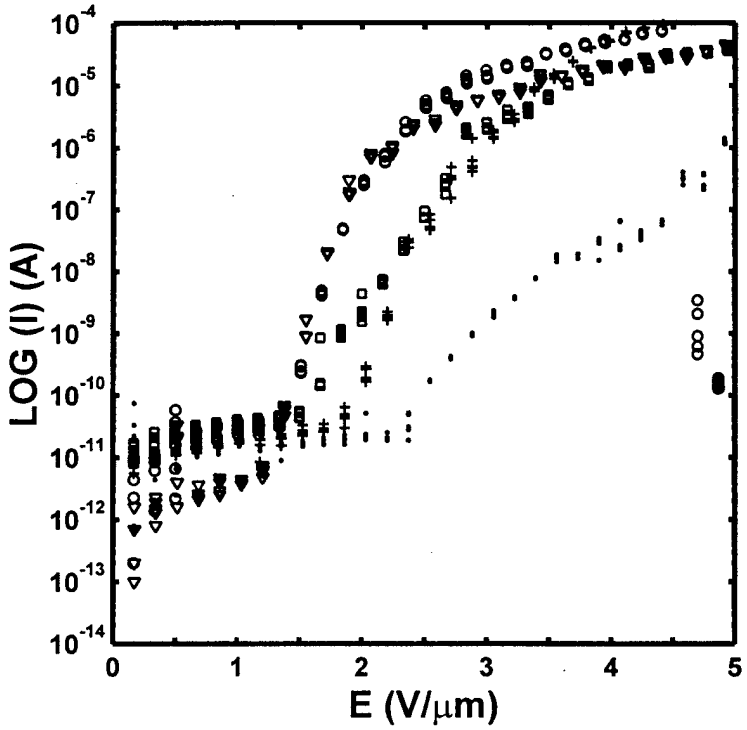

Fig. 7. Electron field emission I-E characteristics of CVD diamond samples deposited using a two-step process in microwave plasmas with methanol to ethanol ratio by weight of (a) 100:10 (dots), (b) 60:30 (triangles), (c) 50:50 (circles), (d) 30:60 (plus signs), and (e) 0:100 (squares), respectively. The nucleation/growth time in minutes were (a) 30/25, (b) 20/9, (c) 25/8, (d) 7/9, and (e) 14/7, respectively.

Proceedings of the Sixth Applied Diamond Conference/Second
Frontier Carbon Technology Joint Conference (ADC/FCT 2001)
Y. Tzeng, K. Miyoshi, M. Yoshikawa, M. Murakawa, Y. Koga,
K. Kobashi, G.A.J. Amaratunga (Editors)

MICROWAVE PLASMA ASSISTED BRAZING OF CARBON NANOTUBES AND DEPOSITION OF CARBON FILMS ON IRON ELECTRODES FOR APPLICATIONS AS ELECTRON FIELD EMITTERS

Yonhua Tzeng, Chao Liu, and Calvin Cutshaw
Alabama Microelectronics Science and Technology Center
Department of Electrical and Computer Engineering
Auburn University, Auburn, Alabama 36849 USA

ASTRACT

Deposition of carbon films including nanotubes as well as brazing of high-quality single wall carbon nanotubes, that were pre-synthesized by other means, on iron electrodes as electron field emitters are reported. Microwave plasmas in vapor mixtures of methanol-based liquid solutions were applied to fresh iron electrodes for carbon and/or carbide deposition. In another application, microwave plasmas were used to heat iron electrodes to its iron-carbon eutectic point around 1150°C so that single wall carbon nanotubes that were placed on the iron surface reacted with iron to form low resistance nanotube-electrode contacts. Electron field emission characteristics of iron electrodes treated by plasma enhanced chemical vapor deposition as well as plasma brazed carbon nanotubes on iron electrodes will be presented.

Keywords: methanol, microwave plasma, electron emission, carbon nanotubes, brazing

INTRODUCTION

Cold and/or low-temperature low-electric-field electron emitters have been studied by a large number of scientists and technologists because of their economic advantages and very attractive performance for many commercial as well as special applications. Devices ranging from high-power microwave vacuum tubes to flat panel displays for computer monitors all require electron emitters that are fast, operating at low temperatures, with high and stable emission current densities at low electric fields.

A number of materials and structures have been studied and reported in an attempt to achieve high-performance cold cathodes. The most effective means of achieving this goal are the fabrication of micro- or nano-structures that exhibit a very high aspect ratio and the design and synthesis of coatings with low positive or even negative electron affinities. The high aspect ratio, for example, a micrometer long carbon nanotube with a nanometer radius of curvature at its tip, allows electric field enhancement to occur at the tip of the electron emitter so that low voltage will be adequate to cause field emission of electrons from the tip of the emitter. Negative electron affinity allows electrons to escape from a solid surface to the vacuum without needing additional forces or energy. For example, diamond with proper surface terminations has been explored for cold cathode applications based on its negative electron affinity. There are a good collection of references in the Proceedings of ADC/FCT '99 (ref. 1) about various efforts, materials, and structures aiming at high-performance electron field emitters.

Several projects have been explored in the past by our research group in collaboration with scientists in the related field. CVD diamond and carbon nanotubes were synthesized and characterized for their electron field emission behaviors (refs 2-10). In an effort to achieve carbon nanotube electron field emitters for high current density and stable electron emission applications, high quality carbon nanotubes may be synthesized separately and then attached to an electrode forming low contact resistance and strong mechanical strength or be directly deposited onto a selected electrode. In this paper, iron electrodes were used because iron serves as an effective catalyst for carbon nanotube growth as well as forms good contacts with carbon materials at its iron-carbon eutectic temperature around 1150°C, which is well below the melting point of iron, so that the electrode remains as a solid at the fabrication temperature (ref. 11).

Diamond deposition in vapor mixtures of methanol-based liquid solutions was reported in ADC/FCT '99 (refs. 12,13). In this paper, microwave plasmas in vapor mixtures of methanol and ethanol were applied to deposit nano-structured carbon coatings on iron electrodes using iron as a catalyst. High-power density microwave plasmas in a vapor of methanol and ethanol were also used to heat and braze single wall carbon nanotubes onto iron electrodes.

EXPERIMENTAL

The experimental apparatus is shown in Figure 1. A mixture of methanol and ethanol was fed into a vacuum chamber that was evacuated by a mechanical pump. A throttle valve and a manometer pressure gauge controlled the chamber gas pressure. A rod antenna was used to couple microwave power from a rectangular waveguide into a cylindrical metal cavity through a quartz window that separated the atmosphere from the vacuum chamber.

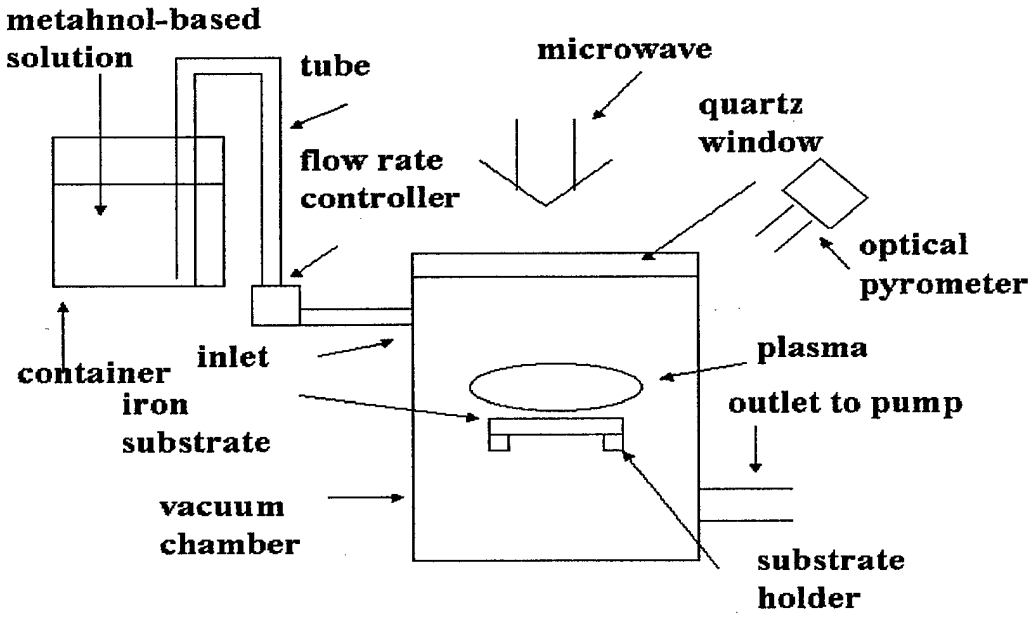

Figure 1. Methanol-based microwave plasma apparatus.

The microwave power formed a plasma ball on the top of the substrate. Electrons in the plasma have very high temperatures exceeding 10,000°C. The plasma heated the substrate to a preset temperature as well as heated the gas mixtures for proper dissociation and reaction in the gas phase leading to carbon deposition on the substrate surface. Iron from the substrate itself was used as the catalyst for the carbon coatings.

In the case of brazing of carbon nanotubes onto iron electrodes, single wall carbon nanotubes suspended in a liquid solution was applied to the surface of an iron electrode. The iron electrode with carbon nanotubes on it was used as the substrate to be exposed to the microwave plasma in a mixture of methanol and ethanol. The substrate temperature was monitored by a dual-color optical pyrometer.

The carbon nanotube coated substrates were then loaded into a high vacuum chamber. Thin quartz plates were used as spacers between an anode and the iron electrode, which serves as the cathode. A desktop computer controlled the output of a high-voltage power supply for applying a voltage between the anode and the cathode. The electric field is calculated by dividing the applied voltage by the gap spacing between the anode and the cathode. The electron emission current was measured by a digital ammeter and recorded by the computer for further plotting and calculation.

RESULTS AND DISCUSSION

Microwave plasmas in methanol-based vapor mixtures with a low percentage of ethanol additives are very oxidizing and can etch carbon nanotubes rapidly at elevated temperatures. Carbon nanotubes placed on molybdenum electrodes were etched away after exposing to microwave plasma in a vapor from a solution of 98% methanol and 2% ethanol by weight at 1250°C for a few minutes. In the case of iron electrodes, carbon nanotubes dissolved into the iron electrode at a temperature above its iron-carbon eutectic temperature in addition to being etched away by the plasma.

Shown in Figure 2 is the electron field emission current-electric field (I-E) characteristics for an iron electrode with carbon nanotube on it before being exposed to the aforementioned microwave plasma for five minutes. The field emission turn-on electric field shows a value above one volt per micrometer, indicating that the electron field emission is not caused by carbon nanotube originally placed on the iron electrode. Indeed, what is shown in Figure 3 is a similar I-E curve for an iron electrode without carbon nanotubes being put on the top before being exposed to the same plasma for the same period of time. SEM images of these two specimens show some sub-micrometer structures on the iron surface that are assumed to be responsible for the measured electron field emission characteristics.

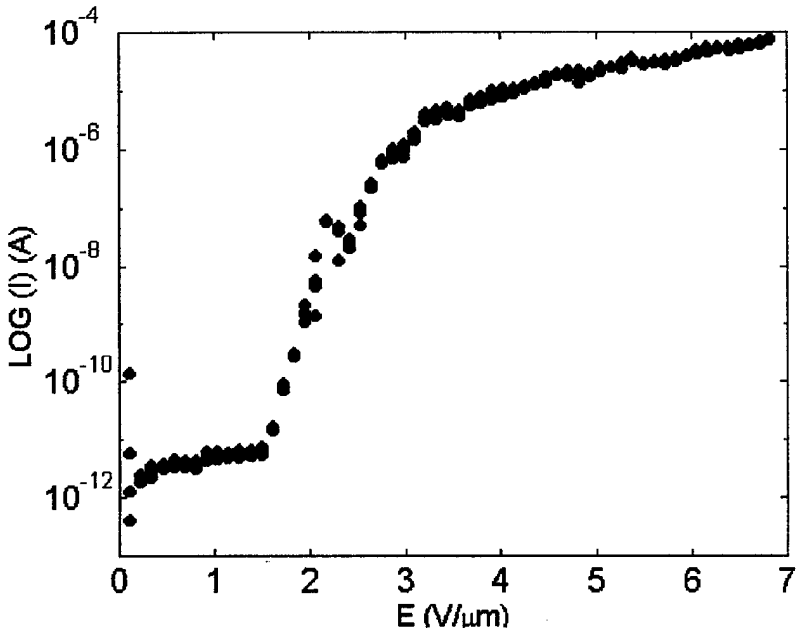

Figure 2. I-E curve for an iron electrode after being exposed to a microwave plasma at 1250C for five minutes. The iron electrode had carbon nanotube placed on it before being exposed to the plasma.

Using a liquid solution with 25% by volume of ethanol in 75% by volume of methanol, a microwave plasma was applied to an iron electrode without pre-synthesized carbon nanotubes on it at 600°C for two hours at a pressure of

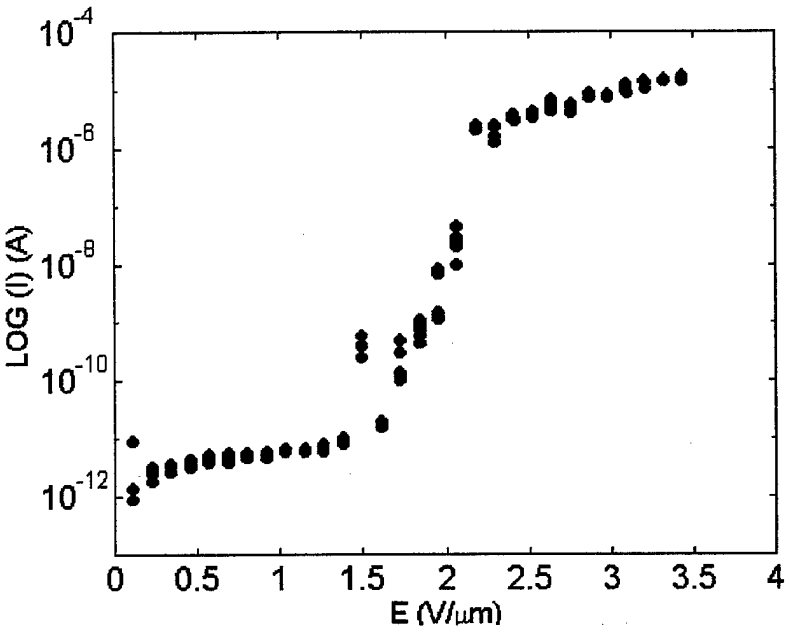

Figure 3. I-E curve for an iron electrode after being exposed to a microwave plasma at 1250C for five minutes.

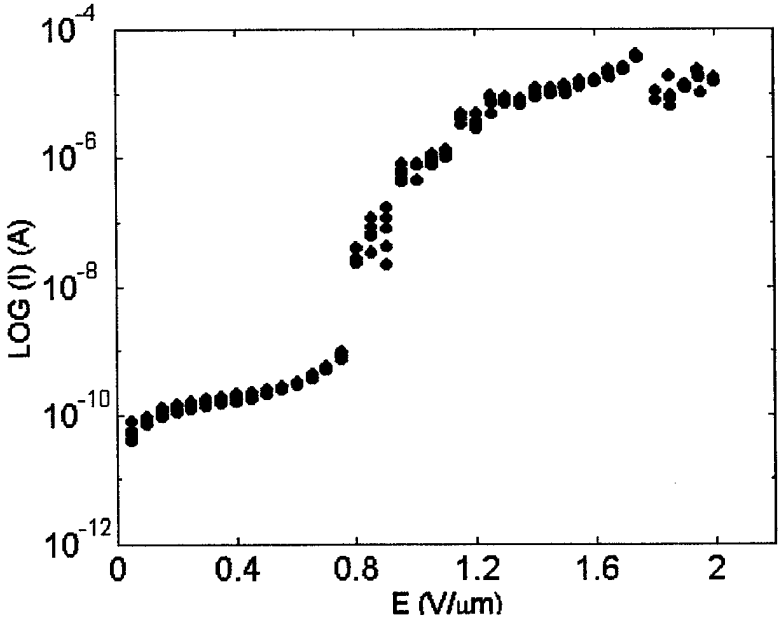

Figure 4. I-E curve for an iron electrode after being exposed to a microwave plasma in 25% ethanol and 75% methanol (by volume) at 600C for 2 hours.

10 Torr. The turn-on electric field shown in Figure 4 for the plasma treated iron electrode was measured to be slightly less than one volt per micrometer. With 25% by volume of ethanol in the liquid solution, the carbon to oxygen ratio was sufficiently high to cause the coatings on the fresh iron electrode, which led to the low electric field electron field emission.

Single wall carbon nanotubes have excellent electron field emission properties. Although it has also been reported that single wall carbon nanotubes can be deposited on substrates directly, it is desirable to be able to optimize the production process for single wall carbon nanotubes independently while the coating process for placing single wall carbon nanotubes on electrodes is separately optimized as well. Brazing of high quality single wall carbon nanotubes to selected electrodes to form a pre-set pattern or structure may be the best strategy.

Using a liquid solution with 25% (by volume) of ethanol in methanol, an iron electrode that had single wall carbon nanotubes placed on its surface was exposed to a microwave plasma at 60 Torr. The greenish plasma heated the iron electrode rapidly to reach above its eutectic temperature within a little more than one minute. A dual-color optical pyrometer was applied to monitor the iron temperature. The plasma was turned off when the iron temperature reached 1160°C, which is slightly above the iron-carbon eutectic temperature. Shown in Figure 5 is the I-E characteristics for the carbon nanotubes brazed onto the iron electrode. A very low electron field emission was measured at macroscopic electric field of less than 0.5 volt per micrometer.

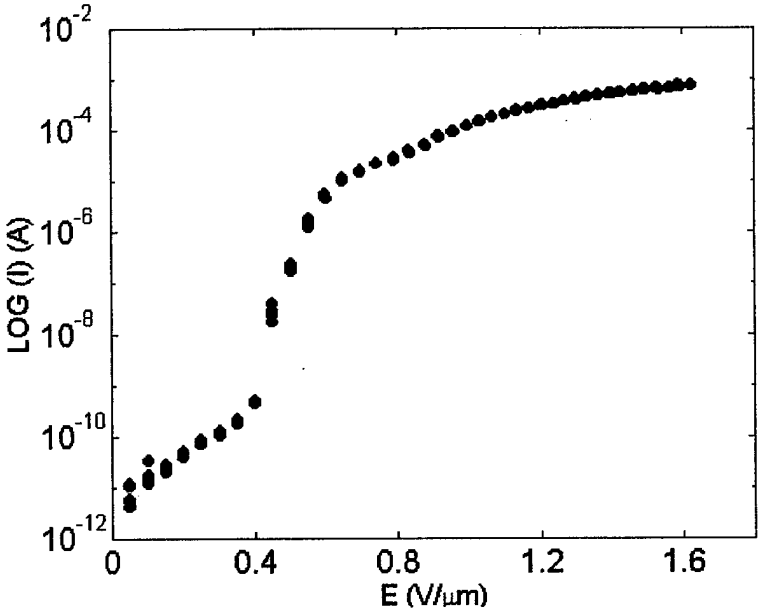

Figure 5. I-E curve for an iron electrode with single wall carbon nanotubes eutectically brazed on it by exposing to a microwave plasma in 25% ethanol and 75% methanol (by volume) until the electrode temperature reached 1160C.

CONCLUSIONS

Methanol-based microwave plasmas were applied to deposit carbon coatings on iron electrodes as well as brazing pre-synthesized single wall carbon nanotubes onto iron electrodes at temperatures near the iron-carbon eutectic temperature. By means of iron-carbon eutectic brazing, electron field emitters are suitable for high current density electron emission applications in which carbon nanotubes may be heated to high temperatures by the emission current. The brazing process also allows the single wall carbon nanotubes to be produced by processes that

are not restricted by the coating process, making it possible for achieving the best performance of electron emitters based on carbon nanotubes.

REFERENCES

1. Yoshhikawa, Y. Koga, Y. Tzeng, C.-P. Klages, K. Miyoshi, editors, *Proceedings of ADC/FCT '99*, pp.335-380 and pp. 687-712, August 31-September 3, 1999, AIST-Tsukuba Research Center, Tsukuba, Japan.

2. N. S. Xu, R. V. Latham, and Y. Tzeng, "Similarities in the `Cold' - Electron Emission Characteristics of Diamond Coated Mo Electrodes and Polished Bulk Graphite Surfaces," J. Phys. D: Applied Physics, 26, pp. 1776-1780, 1993.

3. N. S. Xu, R. V. Latham and Y. Tzeng, "Field-dependence of the Area-density of `Cold' Electron Emission Sites on Broad-Area CVD Diamond Films," Electronics Letters, Vol. 29, No. 18, 2 September 1993.

4. N. S. Xu, Y. Tzeng, and R. V. Latham, "A Diagnostic Study of the Field Emission Characteristics of Individual Micro-Emitters in CVD Diamond Films," J. Phys. D: Appl. Phys. (Rapid Communication) 27, pp. 1988-1991, 1994.

5. N. S. Xu, R. V. Latham and Y. Tzeng. "Field-Induced Electron Emission from CVD Diamond Films on Planar Mo Substrates," Diamond Films and Technology, Vol. 4, No. 4, pp. 249-258, 1994.

6. Yonhua Tzeng, Chao Liu and Zheng Chen, "Hot-Filament Assisted Fabrication of Carbon Nanotube Electron Emitters,", *Mat. Res. Soc. Symp. Proc.* Vol. 621. R7.5.1-R7.5.7, April 24-28, 2000, San Francisco, CA.

7. Zheng Chen, Yonhua Tzeng, Chao Liu, and Calvin Cutshaw, "Fabrication and Applications of Microstructured Ni-C Electrodes with High-Density Carbon- Nanotube Coatings," *Mat. Res. Soc. Symp. Proc.* Vol. 621. R7.4.1-R7.4.4 , April 24-28, 2000, San Francisco, CA.

8. Yonhua Tzeng, Chao Liu, and Zheng Chen, "Electron Emission from Microwave Plasma CVD Carbon Nanotubes," *Mat. Res. Soc. Symp. Proc.* Vol. 621. R7.3.1-R7.3.6 , April 24-28, 2000, San Francisco, CA.

9. Y. Tzeng, C. Liu, and Z. Chen, "Low Temperature CVD Carbon Films on Glass Plates for Flat Panel display applications," *Mat. Res. Soc. Symp. Proc.* Vol. 621. Q2.2.1-Q2.2.5 , April 24-28, 2000, San Francisco, CA.

10. Tzeng, C. Liu, C. Cutshaw, and Z. Chen, "Carbon Nanotube Coatings for Electron Emitter Applications," Presented in the Seventh International Conference on New Diamond Science and Technology, July 24-28, 2000, Hong Kong, China.

11. Y. Tzeng, "Rapid Smoothing of CVD White Diamond by Liquid Metal Films," *Proceedings of the 3rd International Conference on the Applications of Diamond and Related Materials*, NIST, Washington, DC, 1995.

12. Y. Tzeng, "Microwave Plasma Enhanced Chemical Vapor Deposition of Diamond in the Vapor of Methanol-Based Liquid Solutions," *Proceedings of ADC/FCT 1999*, pp.20-24, August 31 –September 4, 1999, Tsukuba, Japan.

13. Y. Tzeng, "Hot-Filament Assisted Deposition of Diamond in the Vapor of Methanol-Based Liquid Solutions," *Proceedings of ADC/FCT 1999*, pp.420-424, August 31 – September 4, 1999, Tsukuba, Japan.

Proceedings of the Sixth Applied Diamond Conference/Second
Frontier Carbon Technology Joint Conference (ADC/FCT 2001)
Y. Tzeng, K. Miyoshi, M. Yoshikawa, M. Murakawa, Y. Koga,
K. Kobashi, G.A.J. Amaratunga (Editors)

HYSTERESIS OF ELECTRON FIELD EMISSION FROM SINGLE-WALLED CARBON NANOTUBES BRAZED ON IRON SUBSTRATES

Chao Liu, Calvin Cutshaw and Yonhua Tzeng
Electrical and Computer Engineering Department, Auburn University
200 Broun Hall, Auburn, Alabama 36849 USA

ABSTRACT

Hysteresis of emission current-electric field (I-E) characteristics of single walled carbon nanotubes brazed on iron substrates by TiCuAg alloy is studied. Different behaviors of the I-E hysteresis with the substrate being held at room temperature and that with the substrate being heated to an elevated temperature were measured. At room temperature, the descending I-E curve was below the ascending I-E curve indicating that tunneling electron emission enhanced by chemisorbed molecules on the surface of the cool carbon nanotube when the emission current first started during the ascending cycle sifts the I-E curve to the upper left. The burn-out of defective or taller carbon nanotubes may also cause the descending I-E curve to shift to the lower right. Both mechanisms may contribute to the measured I-E hysteresis. On the other hand, the I-E hysteresis measured at elevated temperatures showed the descending I-E curve being above the ascending I-E curve. The self-heating of carbon nanotubes by emission current coupled by the less effective cooling with the substrate being at elevated temperatures during the descending cycle, the contribution of thermionic electron emission from nanotubes, and the relatively easier bending and straightening of carbon nanotubes at elevated temperature in alignment with the applied electric field may contribute to the measured I-E hysteresis at elevated temperatures being different from that at room temperature.

Keywords: carbon nanotubes, electron emission, hysteresis, tunneling

INTRODUCTION

Carbon nanotubes are promising for cold cathode applications due to their excellent electrical and mechanical properties, such as high aspect ratio, small tip and curvature, high mechanical strength, and high resistance to chemical and physical attacks (refs. 1 to 4). Various experiments have been carried out and have demonstrated attractively low threshold and turn-on electric fields for field emission of electrons, as well as high emission current densities. Mechanisms for electron emission behaviors of carbon nanotubes are not adequately clear. In this paper, the electron emission characteristics of carbon nanotubes are examined with emphasis on the hysteresis of the emission current-electric field characteristics. The hysteresis of the I-E curves may be related to the stability of the electron field emission in a long-term field emission operation as well as field emission operations under changing environments. The carbon nanotube electron emitter exhibiting the least I-E hysteresis may also be the electron field emitter that will provide the best long-term field emission stability.

EXPERIMENTAL PROCEDURE

The specimen used in this study was prepared by first putting a piece of brazing alloy (Wesgo Ticusil, containing 4.5% Ti, 26.7% Cu, and 68.8% Ag) sheet, which has liquidus phase above 850°C and solidus phase below 830°C, onto a piece of iron with a flat surface. A drop of carbon nanotube suspended in a liquid was then applied onto the brazing alloy sheet. After the liquid vaporized, the specimen was loaded into a vacuum furnace, which was pumped to a pressure of 60 mTorr. The specimen was heated up to 850°C inside the vacuum furnace. The electron emission characteristics of the specimen were measured in a high vacuum chamber under base pressure of 1×10^{-6} Torr. A piece of quartz plate was used as a spacer between the specimen and a counter electrode to control the distance between the anode and the cathode. A potential difference was applied between these two electrodes by a computer controlled power supply. Emission currents were measured by a computer controlled picoammeter. The specimen could be heated to various temperatures up to 860°C during the measurements by using a lamp with an adjustable power supply.

RESULTS AND DISCUSSION

The surface of carbon nanotubes appeared to have been coated with metallic nanoparticles as shown by the SEM photograph (see Figure 1). Figure 2 demonstrates the electron emission hysteresis of the specimen at room temperature. The applying electric field was firstly swept up, and the current was measured as a function of electric field between the anode and the cathode. The electric field was then swept down, and the emission currents were measured to be smaller than those corresponding to the same electric field during the ascending cycle.

Two mechanisms may have contributed to the measured I-E hysteresis. It is known that chemisorbed molecules on a metal surface produce bonding states that have energy levels a few angstroms off the metal surface. These states can increase the local tunneling current by forming a resonant tunneling of electrons (ref. 5). This enhanced electron field emission occurs more significantly when the carbon nanotubes were cool and when the field emission just started at a low level when the electric field is being swept up. It is less effective when the carbon nanotube is cooling down from self-heating by emission current when the applied electric field is swept down. When nanotubes emit electrons with a relatively high current density, the temperature of nanotubes may increase dramatically to a high level (>1000K) due to the self-heating. When the temperature exceeds the desorption temperature for the molecule, the binding states will then be removed. Re-adsorption during the descending cycle may recover some of the chemisorbed molecules. The tunneling enhanced electron emission by chemisorbed molecules, therefore, contributes to the shifting of the ascending I-E curve to the upper left direction.

The second mechanism that may contribute to the measured I-E hysteresis is the burn-out of sticking-out and taller carbon nanotubes. Those taller carbon nanotubes were subjected to higher electric fields and emitted higher electron current densities than those shorter or lower carbon nanotubes. With more current being carried through fewer taller carbon nanotubes, some might be burned away when the applied electric field was swept to the maximum value. When the electric field was swept down (decreasing with time), there were less tall carbon nanotubes and therefore, the I-E curve for the descending cycle shifted to the lower right direction. Both the tunneling effect and the burn-out mechanism appeared to support the measured I-E hysteresis at room temperature with the descending I-E curve being below the ascending I-E curve. The dominant mechanism seemed to be the enhanced tunneling effect due to chemisorbed molecules.

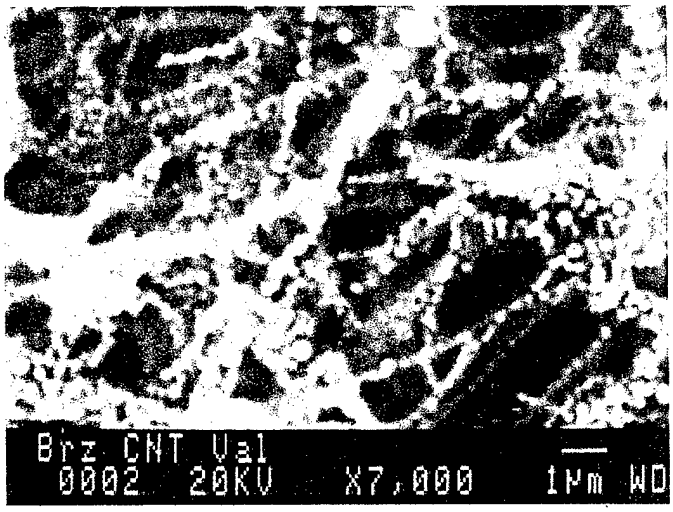

Figure 1. Scanning electron micrograph of brazed single-walled carbon nanotubes on an iron substrate.

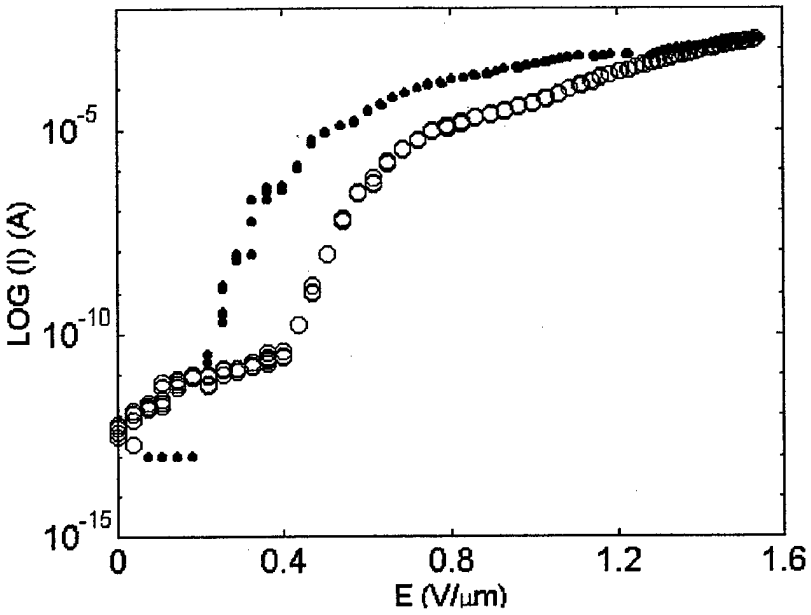

Figure 2. Electron field emission current as a function of applied electric field between the anode and the cathode at room temperature. The dotted curve represents the cycle when the electric field was swept up. The circled curve represents the other cycle when the electric field was swept down.

When the substrate was heated to elevated temperatures, however, the hysteresis behavior of the electron emission I-E curve turned out to be the other way around, i.e., the I-E curve for the descending cycle with decreasing electric field was measured to be above the I-E curve for the ascending cycle (see Figure 3). There should be a thermionic emission component in the total emission current when the electric field was swept up to the maximum level because of the high temperature of nanotubes due to the self-heating effect. When the substrate temperature was at the room temperature, nanotubes could cool down from self-heated high temperature much quicker than when the substrate was heated to an elevated temperature. The contribution by thermionic electron emission may thus be higher during the descending cycle when the substrate was heated to an elevated temperature. The thermionic emission current may have overwhelmed both the chemisorbed molecule enhanced tunneling current and the current changing due to the burn-out of electron emitting nanotubes resulting in the hysteresis behavior shown in Figure 3.

Stepwise increases in electron emission current were sometime observed when the substrate was heated to elevated temperatures (see Figure 4). This may be a result of the increasing flexibility and weaker bonding of nanotubes leading to easier alignment of carbon nanotubes with the applied electric field causing the electron emission current to change suddenly. As temperature increased, the bonds that kept nanotubes from being aligned with the electric field became weaker. Therefore, when the temperature was high enough, it was possible that one end of a CNT became free from the substrate surface and that this CNT was bent to align with the applied electric field. The changing of the height of the tips of electron emitting carbon nanotubes might have contributed to the stepwise increase and decrease of the emission currents. As shown in Figure 1, there was quite a coating of metallic nanoparticles on the nanotubes. This coating may also contribute to the hysteresis of the I-E characteristics and the step-wise changes of electron emission current. Further investigation is underway to explore the effects of coatings on carbon nanotubes on electron field emission.

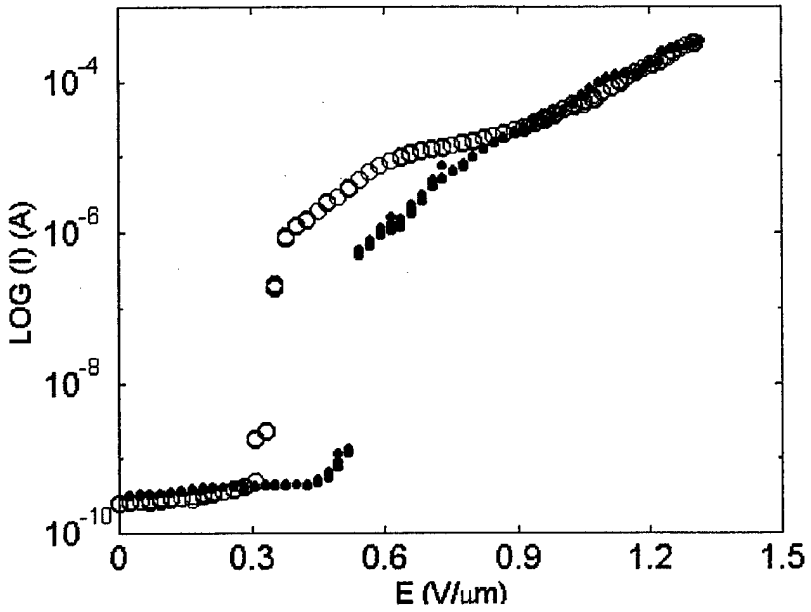

Fig. 3. Electron emission current as a function of applied electric field between the anode and the cathode with the substrate being heated to above 500°C. The dotted curve represents the cycle when the electric field was swept up while the circled curve represents the cycle when the electric field was swept down.

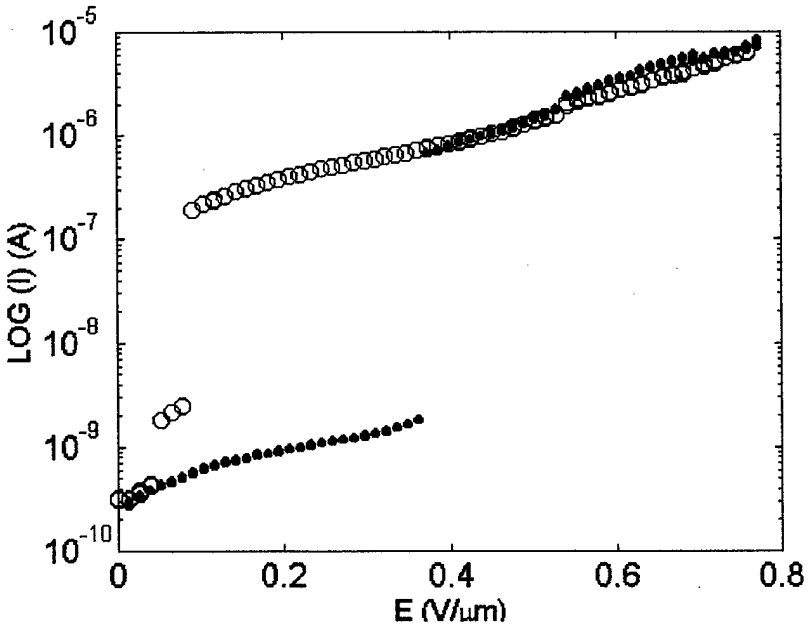

Fig. 4. Electron field emission current as a function of applied electric field between the anode and the cathode with the substrate being heated to above 500°C. The dotted curve represents the ascending cycle when the applied electric field increased with time. The circled curve represents the descending cycle when the electric field decreased with time.

CONCLUSIONS

Five mechanisms were adopted to explain the hysteresis of I-E characteristics of the electron field emission from carbon nanotubes brazed by a TiCuAg alloy to an iron substrate. Those five mechanisms play different roles during the electron emission of carbon nanotubes. At low ambient temperatures, the chemisorbed molecule enhanced tunneling may be the dominant mechanism. The burn-out of nanotubes is negligible in most cases especially after carbon nanotubes have been "conditioned", that is, defective or tallest carbon nanotubes have been intentionally removed, because long term testing of emission current demonstrates a fairly stable emission current, indicating that the damaging of emission sites are small (ref. 2). At higher ambient temperatures, however, because of the removal of chemisorbed molecules on the nanotube surfaces, the contribution by thermionic emission and the relaxation of nanotubes to align with the applied electric field might become dominant forces pushing the hysteresis of I-E curves to a direction opposite that for substrate being at low temperatures. The sharp, sometimes stepwise, increases of emission current might be the consequence of the changing shapes of the nanotubes in alignment with the electric field as well as the absence of chemisorbed molecule enhanced electron emission by tunneling.

REFERENCES

1. Yahachi Saito and Sashiro Uemura: "Field emission from carbon nanotubes and its application to electron sources", Carbon, 85, 7, 2000, p169.
2. W. Zhu et al.: "Large current density from carbon nanotube field emitters", Appl. Phys. Lett., 75, 6, 1999, p873.
3. O. Gröning et al.: "Field emission properties of carbon nanotubes", J. Vac. Sci. Technol. B, 18(2), 2000, p665.
4. R. Saito, G. Dresselhaus, and M. S. Dresselhaus: Physical Properties of Carbon Nanotubes, Imperial College Press, London, 1999 Journal of Applied Physics, Volume 85, Number 7, 1999, p3832.
5. Kenneth A. Dean and Babu R. Chalamala: "Field emission microscopy of carbon nanotube caps", J. Appl. Phys., 85, 7, 1999, p3832.